

87  
6-14-76  
- copy to NTIS

# Lawrence Livermore Laboratory

THE BATTERY-FLYWHEEL HYBRID ELECTRIC POWER SYSTEM FOR NEAR-TERM APPLICATION  
VOLUME 2 - SYSTEM DESIGN

D. D. Davis )  
L. G. O'Connell ) Lawrence Livermore Laboratory  
S. E. Warner )  
A. E. Raynard )  
B. H. Rowlett ) Airesearch Manufacturing Company

April 15, 1976



This is an informal report intended primarily for internal or limited external distribution. The opinions and conclusions stated are those of the author and may or may not be those of the laboratory.

Prepared for U.S. Energy Research & Development Administration under contract No. W-7405-Eng-48.



**MASTER**

DISTRIBUTION OF THIS DOCUMENT IS UNLIMITED

## DISCLAIMER

**This report was prepared as an account of work sponsored by an agency of the United States Government. Neither the United States Government nor any agency Thereof, nor any of their employees, makes any warranty, express or implied, or assumes any legal liability or responsibility for the accuracy, completeness, or usefulness of any information, apparatus, product, or process disclosed, or represents that its use would not infringe privately owned rights. Reference herein to any specific commercial product, process, or service by trade name, trademark, manufacturer, or otherwise does not necessarily constitute or imply its endorsement, recommendation, or favoring by the United States Government or any agency thereof. The views and opinions of authors expressed herein do not necessarily state or reflect those of the United States Government or any agency thereof.**

## **DISCLAIMER**

**Portions of this document may be illegible in electronic image products. Images are produced from the best available original document.**

THE BATTERY FLYWHEEL HYBRID ELECTRIC POWER SYSTEM  
FOR NEAR-TERM APPLICATIONS

Table of Contents

VOLUME II -- SYSTEM DESIGN

Foreword

I.	Flywheel Design	
A.	Flywheel Sizing	1
B.	Flywheel Baseline Design	14
C.	Flywheel Safety	21
II.	Power Transmission Design	
A.	Electromechanical Transmission	25
B.	Traction Motor and Flywheel Motor	30
III.	Control System Design	
A.	Component Description	35
B.	Operational Mode Control	43
IV.	Performance Calculations	
A.	Rationale	50
B.	Vehicle Descriptions	51
C.	Definitions	52
D.	Calculations	61
E.	Range Calculation Summary	71
F.	Grade and Acceleration Performance	72

References

**NOTICE**  
This report was prepared as an account of work sponsored by the United States Government. Neither the United States nor the United States Energy Research and Development Administration, nor any of their employees, nor any of their contractors, subcontractors, or their employees, makes any warranty, express or implied, or assumes any legal liability or responsibility for the accuracy, completeness or usefulness of any information, apparatus, product or process disclosed, or represents that its use would not infringe privately owned rights.

DISTRIBUTION OF THIS DOCUMENT IS UNLIMITED

*leg*

## FOREWORD

This is the second of two volumes which document the result of an investigation of Battery-Flywheel Power Systems. Volume I is, "The Battery Flywheel Hybrid Electric Power System for Near Term Applications"-- System Description.

SECTION I

FLYWHEEL DESIGN

A. FLYWHEEL SIZING

Flywheel sizing must be accomplished by an interactive study of vehicle mission and performance, propulsion system parameters, and flywheel design characteristics. This process can be used for a range of vehicles employing either flywheel hybrids or pure flywheel systems. The interactive study factors to be considered are shown in Table 13. The energy storage requirements are determined by summing the energy requirements for the vehicle mission (or missions) and the inefficiencies that occur in the propulsion system components.

A prime factor in sizing the flywheel is the energy density of the flywheel rotor. Another big factor is the consequent effect of the rotor design on the container design. Tests and studies made to date show the need for obtaining high-energy densities in flywheel propulsion systems. A comparison of various flywheel designs and their relation to energy density is shown in Figure 14. The total system weight includes the sum of rotor weights and the container weight. The technique of reducing the amount of kinetic energy stored in any one element through the use of a multidisk design greatly reduces the weight of the containment ring.

Composite material rotors provide a large payoff in both rotor energy density and in reduction of container weight. However, any tradeoff comparison between the use of steel and composite materials for the rotor must consider the relative state of development of both materials.

The flywheel energy density can be expressed as:

$$\frac{KE}{W} = K_S \frac{\sigma}{Y}$$

TABLE 13  
FLYWHEEL SIZING TRADEOFF STUDY

---

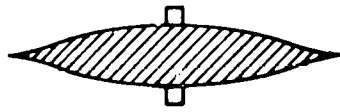
FLYWHEEL SIZING FACTOR	PARAMETRIC CONSIDERATION
Vehicle mission and performance performance	Vehicle range, weight, number of stops, regeneration, auxiliary loads, road load, flywheel losses, propulsion system round trip efficiency
Rotor energy density	Rotor type, material peripheral speed, rotor attachment
Containment/rotor weight ratio	Rotor type, material, energy amount per disk containment ring material thickness
Input/output power unit	Speed ratio, efficiency vs. load and speed, charging time
Flywheel design	Envelope limits; bearing, windage; seal and gear losses; rotational speed, gyrodynamic loads

---

## METAL FLYWHEEL CONFIGURATIONS

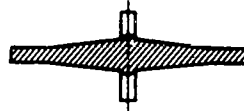
$$\frac{KE}{WT} = K_S \frac{\sigma}{\gamma}$$

$\sigma$  = ALLOWABLE STRESS  
 $\gamma$  = WEIGHT DENSITY  
 $K_S$  = MEASURE OF MASS UTILIZATION OF MATERIAL (SHAPE FACTOR)



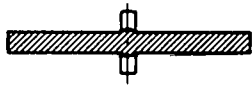
(a) CONSTANT STRESS DISC

$$K_S = 1.0$$



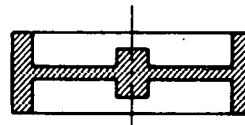
(b) SHAPED DISC

$$K_S = 0.9 \text{ TYP}$$



(c) FLAT DISC

$$K_S = 0.606$$



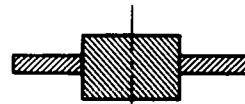
(d) RIMMED DISC

$$K_S = 0.4 \text{ TYP}$$



(e) FLAT DISC WITH HOLE

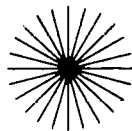
$$K_S = 0.303$$



(f) FLAT DISK SHRUNK ONTO HUB

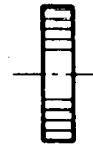
$$K_S = .303$$

## COMPOSITE FLYWHEEL CONFIGURATIONS



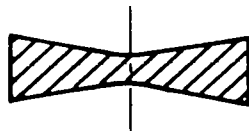
RADIAL FIBERS DISC, BAR

$$K_S = .35$$



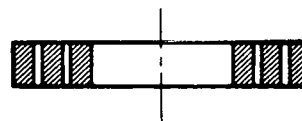
CIRCULAR WOUND DISC,  
THICKWALL CYLINDER

$$K_S = .303$$



RADIAL/CIRCULAR FIBER DISC

$$K_S = .45$$



MULTIPLE CONCENTRIC RINGS

$$K_S = .40$$

Figure 14 Flywheel configurations



where:

KE = kinetic energy

W = weight

$\sigma$  = allowable stress

$\gamma$  = weight density

$K_s$  = nondimensional shape factor

Values of  $K_s$  for various flywheel geometries are shown in Figures 14 and 15.

The energy density determination for a flywheel rotor is the product of flywheel shape factor and the allowable stress-to-weight density ratio. These relationships are also shown in Figure 15. The flywheel shape factor,  $K_s$ , can be used as a guide for rotor design, but the other flywheel sizing factors have to be carefully traded off to arrive at an optimum solution for a specific application or vehicle performance requirement.

#### Flywheel Materials

In the selection of materials for the rotor, considerable emphasis must be placed upon the utilization of established materials that have the best attainable combination of the following characteristics:

- High yield and ultimate strength
- High fatigue strength (endurance limit)
- Good fracture toughness (flaw tolerance) at operating and subzero temperature
- Low fatigue crack propagation rate
- Uniformity of mechanical properties in thick sections
- Adequate corrosion resistance
- Reasonable cost
- History of prior usage as a flywheel material

EQUAL FATIGUE MARGIN DESIGNS	LAMINATED ROTOR (SHRINK FIT)	SHAPED DISC	MULTI-DISC TIE-BOLTS	MULTI-DRUM	MULTI-DRUM	MULTI-DRUM
MATERIAL	STEEL	STEEL	STEEL	S-GLASS	KEVLAR	GRAPHITE
SHAPE FACTOR $K_S$	0.30	0.85	0.43	0.35	0.35	0.35
MAX. STRESS/DENSITY (IN.-LB/LB)	590,000	490,000	530,000	2,280,000	3,270,000	2,240,000
PERIPHERAL SPEED (FT/SEC)	1360	2300	1720	2470	3000	2450
DIAMETER/LENGTH	1.0/1.0	1.70/0.51	1.26/0.89	1.82/0.24	2.20/0.14	1.79/0.32
ROTATIONAL SPEED	1.0	1.0	1.0	1.0	1.0	1.0
ROTOR WEIGHT (RELATIVE)	1.0	0.42	0.78	0.22	0.15	0.23
APPROX. CONTAINMENT WEIGHT	0.3	1.3-1.4	0.3-0.4	0.2-0.4	0.2-0.4	0.2-0.4

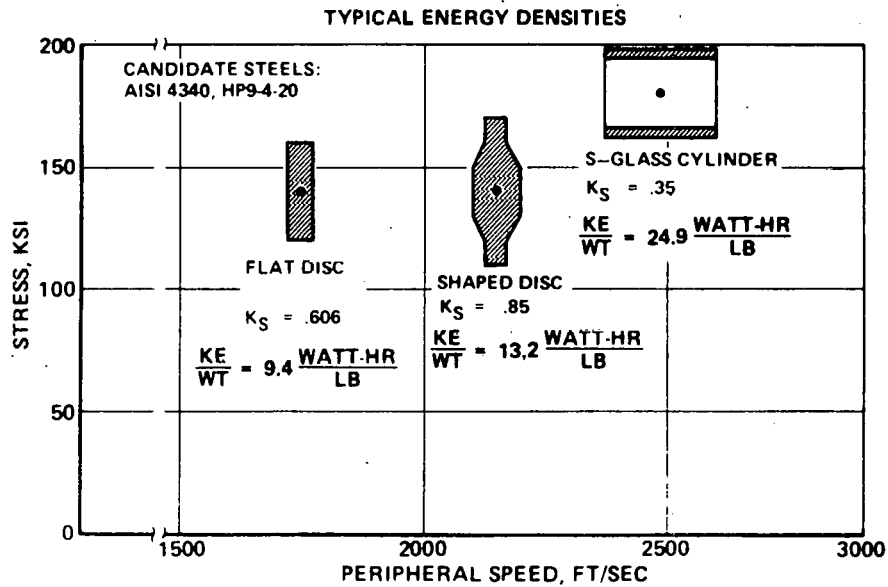


Figure 15 Flywheel comparisons

### Steel Materials

The minimal requirements that must be satisfied by a steel rotor material are high yield strength, high fatigue strength, and good fracture toughness. The ultra-high strength steels possessing this combination of properties usually are very sensitive to variations in composition, thermal and mechanical processing, and degree of cleanliness of the material. Therefore, careful nondestructive inspection techniques are required to provide the degree of quality assurance needed.

### Composite Materials

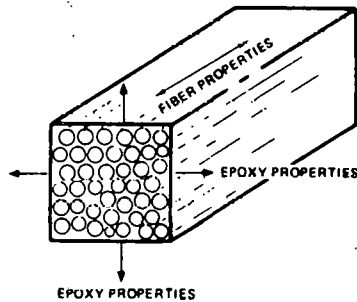
In addition to homogeneous metal rotor materials, composite structures consisting of high-strength fibres held together by a binder such as epoxy resin offer potential for flywheel rotors. The advantages of composite include: (1) reduction in rotor containment weight, (2) competitive manufacturing cost, and (3) high strength-to-weight density, which allows higher operating speeds and hence a reduction in rotor weight. Disadvantages include: (1) delamination of thick sections on spinup because of low radial strength and large radial growth, (2) difficulty in connecting the composite structure to the rotor shaft, and (3) relatively low specific energy per unit volume compared to metal rotors.

Whether or not filament-epoxy type should be used in any specific design will depend on the combined requirements of energy density, energy volume, and rotor cost. Practical rotor designs have been made from E-glass, S-glass, and Kevlar-epoxy combinations. Candidate materials are shown in Figure 16.

## MATERIALS FOR FLYWHEEL APPLICATIONS

MATERIAL	ULTIMATE TENSILE STRENGTH, KSI	"USABLE" TENSILE STRENGTH, KSI		DENSITY LB/IN.	STRENGTH/DENSITY IN.-LB/LB x 10 <sup>6</sup>		RAW MATERIAL COST \$/LB	RELATIVE RATING STRESS DENSITY / COST IN.-LB/\$ LONG TERM
		LONG TERM	SHORT TERM		LONG TERM	SHORT TERM		
<b>STEELS</b>								
4340 STEEL	220	140	160	0.283	0.49	0.56	0.90	0.54
HP 9-4-20	200	140	160	0.284	0.49	0.56	2.90	0.17
18 Ni (300)	300	150	200	0.289	0.52	0.69	6.00	0.09
<b>COMPOSITES</b>								
E-GLASS EPOXY	200	120	150	0.080	1.50	1.87	1.20	1.25
S-GLASS EPOXY	300	180	225	0.079	2.28	2.84	1.90	1.20
KEVLAR-EPOXY	280	170	210	0.052	3.27	4.04	4.80	0.68
GRAPHITE-EPOXY	230	140	170	0.058	2.41	2.93	44.00	0.06

## FILAMENT-EPOXY MATRIX PROPERTIES



● **USABLE FIBER STRENGTH (COMPOSITE)**

"E" GLASS 120,000 PSI,  $\rho = 0.080$  LB/IN.<sup>3</sup>  
 "S" GLASS 180,000 PSI = 0.079  
 KEVLAR 170,000 PSI = 0.052

● **USABLE EPOXY STRENGTH 3,000 PSI**

● **COMPOSITE PROPERTIES VARY DEPENDING UPON % FIBER IN MATRIX**

Figure 16 Flywheel materials

### Dynamic Considerations

a) Critical Speeds. Because of the relatively heavy rotor and the inherent upper limit in radial stiffness of antifriction bearings, the flywheel rotors usually will have at least one critical speed below rated speed. These critical speeds essentially will be rotor rigid body modes with the primary flexibility occurring in the bearings and bearing supports. The rotor and shafts and disk connections must be designed to result in a stiff rotor. If necessary, the rigid body critical speeds can be positioned by using specially designed resilient bearing supports.

b) Torsional Analysis. A transient torsional analysis of the system is required to assure system stability and determine transient torques in the torque transmission system. The characteristics of the flywheel transmission must be established to perform this analysis.

c) Rotor Balance. Provisions must be made to balance the rotor to minimize unbalance loads on the bearings and supporting structure. The flywheel rotor will be relatively rigid and therefore a final two-plane balance of the assembled rotor will be sufficient. This unbalance must be equivalent to less than 0.0001 in. eccentricity. If a multidisk rotor is used, balance of each individual disk must be accomplished to minimize the balancing of the assembled rotor.

### Gyroscopic Effects

The flywheel will possess a large angular momentum when in operation. Any change in the angular momentum vector by a rolling or yawing velocity will create large gyroscopic moments that must be reacted by the flywheel rotor

bearings and associated bearing support structure. The bearings and support structure must be designed to accommodate these loads.

The rotor gyroscopic moments ( $M_G$ ) are given by:

$$M_G = I \cdot \omega \cdot \Omega$$

where

$I$  = polar moment of inertia

$\omega$  = rotational speed

$\Omega$  = precessional velocity of the axis of rotation

The gyroscopic bearing reactions ( $R_G$ ) are given by:

$$R_G = M_G L$$

where

$L$  = bearing span

A more general form of the bearing reactions can be expressed in terms of the energy (KE) stored in the flywheel as

$$R_G = \frac{KE}{V} \left( \frac{Do}{L} \right) \Omega$$

where

KE = flywheel kinetic energy

$V$  = flywheel rim peripheral speed

Do = flywheel outside diameter

Therefore, assuming

$$KE = 1 \text{ kwhr} = 2.65 \times 10^6 \text{ ft-lb}$$

$$V = 2830 \text{ fps}$$

$$\Omega = 0.5 \text{ radians}$$

$$R_G = \frac{2.65 \times 10^6}{2870} \text{ Do/L} (0.5)$$

$$R = 462 \text{ Do/L lb}$$

As shown above, the bearing reactions depend upon the diameter-to-bearing span ratio ( $D_o/L$ ). This ratio in turn primarily is governed by the design rotational speed. Higher design speeds will result in a smaller diameter and longer rotor and therefore lower bearing reactions. The following table shows the approximate bearing reactions for a range of design speeds and an assumed precession rate of 0.5 radians per second.

N, rpm	18,000	36,000
$D_o/L$	6	2
R (lb)	2770	924

The design value of precession rate must be established and will depend on the orientation of the flywheel spin axis with respect to the angular velocity vector. For example, if the spin axis were oriented horizontal and transverse to the longitudinal axis of a vehicle, the pitching velocity (which can be large over rough terrain) would not cause any gyroscopic loads on the flywheel. The bearing support structure and bearings must be designed to accommodate these gyroscopic loads.

#### Friction Losses

The major factors to be considered in the flywheel module are the rotor bearing losses. Windage losses can be reduced substantially by providing a vacuum in the flywheel cavity of 5 microns, Hg. The rotor bearings then become the major loss contributor to the flywheel module. A preliminary calculation of flywheel module losses has been made and is shown in Table 14.

Table 14  
Friction Losses at 100-Percent RPM

<u>Item</u>	<u>Loss, watts</u>
Windage	100
Rotor bearings (2)	120
Rotor seal	80
Lube and vacuum pump	80
Total:	380

#### Windage Losses

Flywheel rotor windage losses can be minimized effectively by providing a vacuum environment in the regime illustrated in Figure 17. Flywheel systems operate at vacuum levels in the range of 10 mm Hg (10 torr), typical of flywheels operating at peripheral speeds of 1100 ft/sec. If the flywheel rotor design permits operation at increased peripheral speeds, the windage losses increase rapidly as shown in Figure 17. Therefore, high peripheral speeds demand the use of vacuum environments in the range of 1 to 1000 microns ( $10^{-3}$  to  $10^{-1}$  torr). The windage loss vs. vacuum relationship is illustrated in Figure 17 for a typical flywheel rotor of 2510 ft/sec peripheral speed.

#### Bearing Losses

Bearing losses can be minimized by the use of rolling element bearings with properly designed separators. The lowest possible rolling element tangential velocity consistent with load capacity should be achieved. The largest variable in bearing loss is in the method of bearing lubrication. Typical bearing losses are shown in Figure 18.



Design considerations

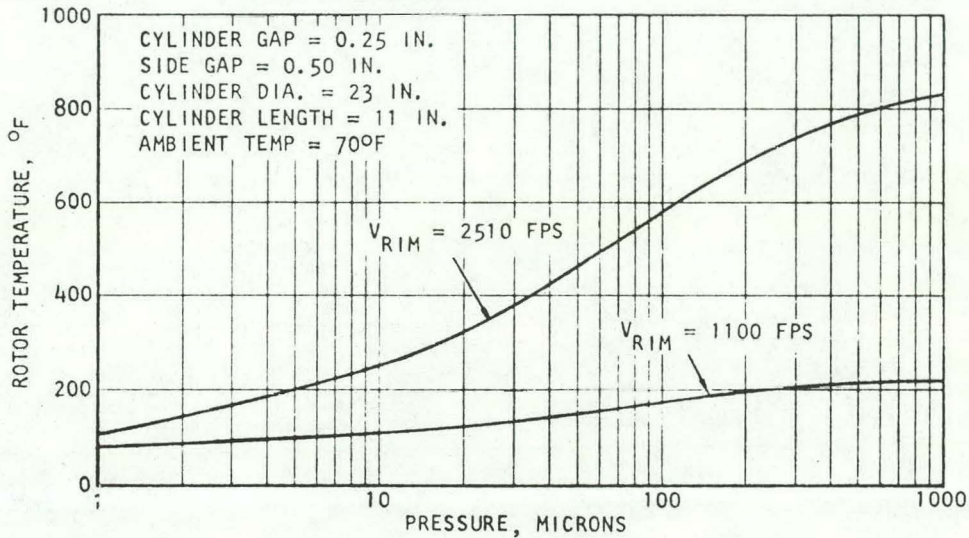
Input

- Rotor peripheral speed
- Cavity gas - density and viscosity, gas dynamic regime
- Rotor rim and side clearances
- Rotor shape

Output

- Rotor and housing temperatures
- Heat balance and drag losses

Typical rotor windage temperature



Typical rotor windage loss

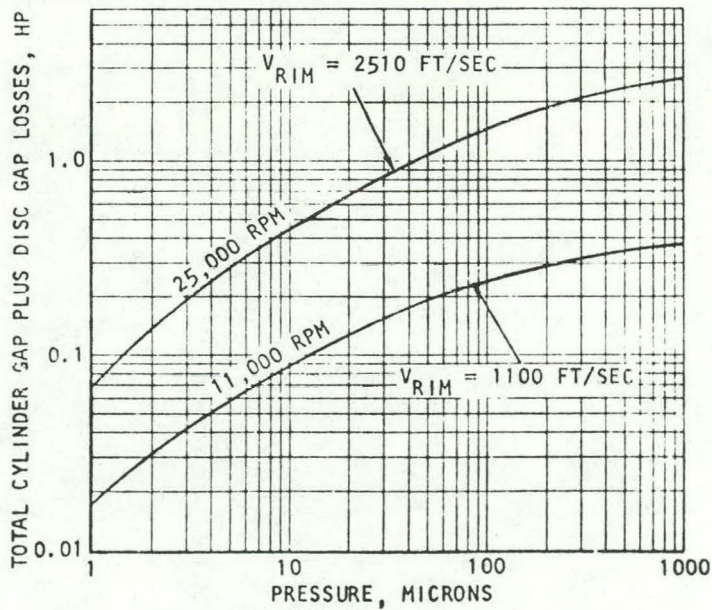


Figure 17 Typical flywheel windage analysis

## BEARING TRADEOFF STUDY

DESIGN CONSIDERATION	PARAMETRIC INVESTIGATION	INVESTIGATIVE METHOD
EXTERNAL LOADS AND INTERNAL BEARING CONSTRUCTION.	BEARING SIZE, WEIGHT, BEARING LIFE. ROLLING ELEMENT: ROLLER OR BALLS, SHAPE AND CONTACT PARAMETERS.  RACES: CURVATURE AND RADIAL CLEARANCES.  MOUNTING FIT, PRELOAD AND RESILIENT SUPPORT	COMPUTER ANALYSIS: 5 DEGREE OF FREEDOM PROGRAM  SYSTEM ANALYSIS - INPUT: ALL DESIGN PARAMETERS.  TESTS ON TEST RIG TO CONFIRM ANALYSIS. EXPERIENCE, RELATED APPLICATIONS.
MATERIAL SELECTION -- ROLLING ELEMENTS	ENVIRONMENTAL FACTORS, SPEED + LOADS DETERMINE MATERIAL SELECTION. PREMIUM 52100, 440C, M50 STEELS.	EXPERIENCE, TEST DATA AVAILABLE FROM RELATED PROGRAMS.
SEPARATOR	BRONZE OR STEEL, INNER OR OUTER RACE CONTROL, SURFACE TREATMENT	
LUBRICATION AND COOLING	COOLING REQUIREMENTS, LUBRICATION METHOD -- JET, MIST, SPLASH  LOSSES DUE TO VISCOUS EFFECT OF LUBRICANT, LOAD AND SPEED.  LUBRICANT TYPE: ENVIRONMENT, LIFE, COST.	COMPUTERIZED THERMAL ANALYSIS TESTS WITH EXTERNAL BEARING COOLING.  EXPERIENCE, RELATED APPLICATIONS.

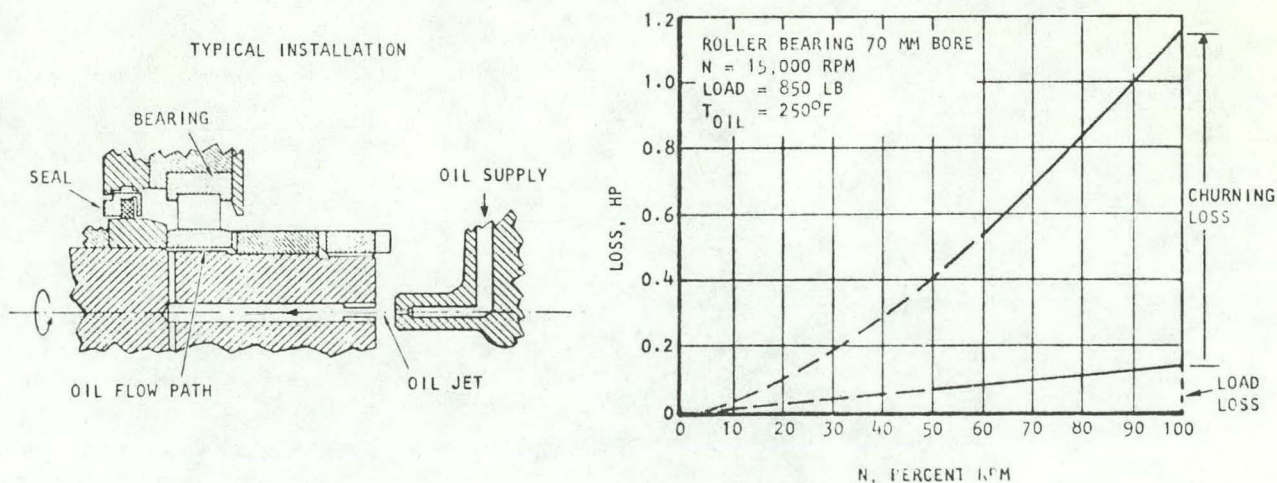


Figure 18 Bearing loads and losses



## B. FLYWHEEL BASELINE DESIGN

### Rotor

For the hybrid power system, a baseline design flywheel was selected that has a total energy capacity of 1 kw-hr. The net energy available for release will be 750 watt-hours over an operating speed range of 40,000 to 20,000 rpm.

The rotor is constructed of Kevlar 49-epoxy composite material in a concentric ring design. The rotor is 18 inches in diameter by 5 inches wide and weighs 34 lbs. The energy density of the rotor is 30 Whr per lb. The selected rotor configuration is shown as concept H on Figure 19. Figure 20 is a representation of the rotor to be used.

### Flywheel Housing

The flywheel housing is very critical, not only because it forms the mounting and containment structure for all the rotating components, but also because slight changes in design can have a significant effect upon the weight of the unit since such a large surface area is involved. The housing with bearings and seal is estimated to weigh 15 pounds.

The entire flywheel housing will be mounted to the vehicle with mount rings that permit rotation of the energy storage unit within the mount rings. As a result, the loads transferred to the structure in the event of a rapid momentum transfer from the rotor to the housing will be limited to acceptable levels. This design technique is used in the ACT-1 (Advanced Concept Train) flywheel and input/output machine.

### Rotor Bearings

A combination of a ball bearing and a roller bearing can be used to support the flywheel rotor. The ball bearing will provide radical load capability for the rotor gravity load.

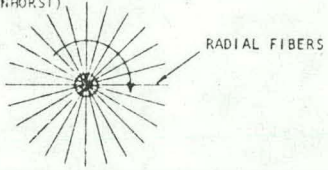
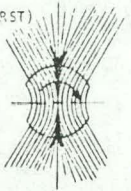
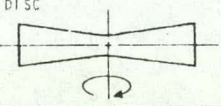
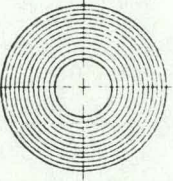
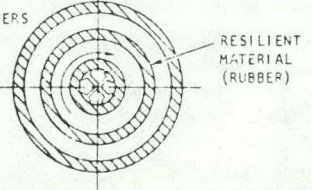
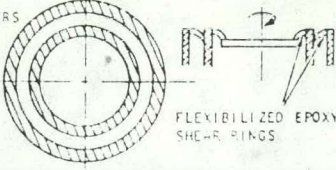
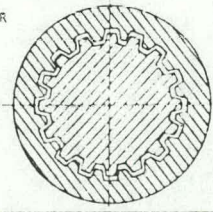
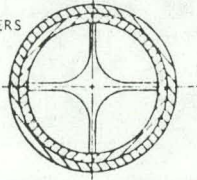
CONFIGURATION	ADVANTAGES	DISADVANTAGES	RELATIVE RATING, $K_s$
<p>CONCEPT A RADIAL BRUSH (RABENHORST)</p> 	<p>UTILIZE FULL FIBER STRENGTH POSSIBLE TO ATTACH TO HUB</p>	<p>HIGH VOLUME HIGH SPEED NO PRACTICAL CENTER ATTACHMENT</p>	<p>MAXIMUM 0.33</p>
<p>CONCEPT B FINNED BRUSH (RABENHORST)</p> 	<p>UTILIZE NEARLY FULL FIBER STRENGTH POSSIBLY A PRACTICAL HUB ATTACHMENT</p>	<p>HIGH VOLUME HIGH SPEED DIFFICULT TO FABRICATE</p>	<p>0.30</p>
<p>CONCEPT C RADIAL/CIRCULAR DISC (POLAR WEAVE)</p> 	<p>HIGH SHAPE FACTOR UTILIZE NEARLY FULL FIBER STRENGTH LOW VOLUME</p>	<p>PLANE STRAIN EXCEEDS COMPOSITE TRANSVERSE STRENGTH</p>	<p>0.45</p>
<p>CONCEPT D CIRCULAR WOUND DISC</p> 	<p>SIMPLE HUB ATTACHMENT LOW VOLUME</p>	<p>HIGH RADIAL STRESS EXCEEDS COMPOSITE STRENGTH</p>	<p>0.30</p>
<p>CONCEPT E CONCENTRIC CYLINDERS (POST &amp; POST)</p> 	<p>UTILIZE FULL FIBER STRENGTH LOW VOLUME</p>	<p>NO SUITABLE RESILIENT MATERIAL AT SPEED, BALANCE PROBLEM</p>	<p>0.35</p>
<p>CONCEPT F CONCENTRIC CYLINDERS (BROBECK)</p> 	<p>UTILIZE FULL FIBER STRENGTH LOW VOLUME</p>	<p>SHEAR RINGS NOT DEMONSTRATED AT SPEED, BALANCE PROBLEMS</p>	<p>0.35</p>
<p>CONCEPT G NOTCHED CYLINDER (BROBECK)</p> 	<p>UTILIZE NEARLY FULL FIBER STRENGTH</p>	<p>HIGH HUB WEIGHT AT SPEED, BALANCE PROBLEMS NOTCHES DEADWEIGHT ON CYLINDER</p>	<p>0.35</p>
<p>CONCEPT H CONCENTRIC CYLINDERS (AIRSEARCH)</p> 	<p>UTILIZE FULL FIBER STRENGTH REASONABLE VOLUME DEMONSTRATED 1000 CYCLES</p>	<p>HIGH LOCAL BENDING STRESS AT SPOKES</p>	<p>0.40</p>

Figure 19 Composite flywheel design comparisons

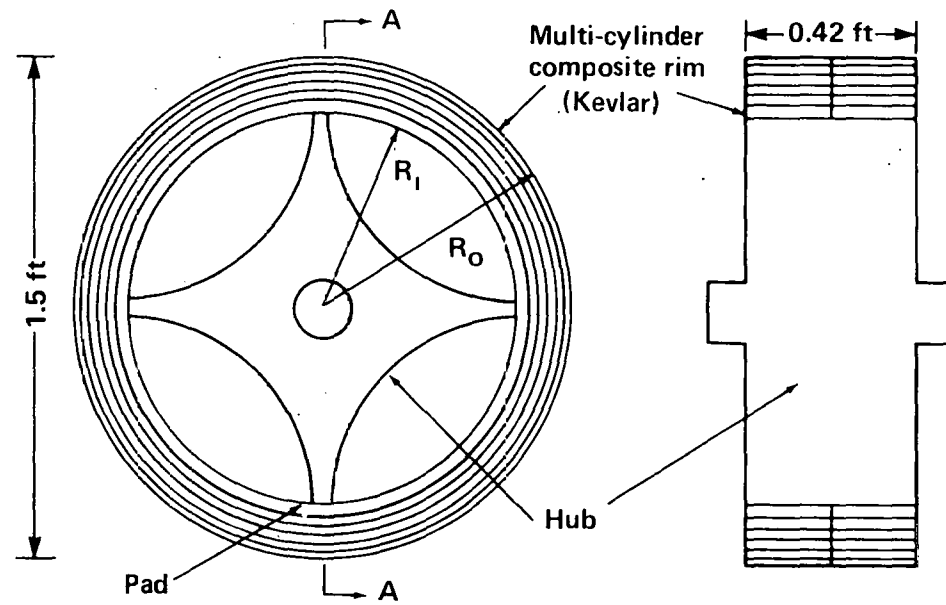


FIGURE 20.. Composite flywheel configuration.

The flywheel bearings size is such as to achieve speeds of approximately 1 million DN (bore size in mm x rpm). The rings and rollers are to be made from 52100 steel, which has adequate strength and hardness at the design operating temperatures. The design objective is to have approximately 100,000-hr B10 fatigue life for the bearings. This provides a generous margin for any unforeseen loading or operating conditions.

Roller bearings are capable of operating under heavy radial loads; however, their ability to withstand misalignment or thrust loads is somewhat limited. The roller separator is expensive to machine because of the square or rectangular pockets and the requirement for roller retention. However, the use of a roller bearing facilitates the assembly and disassembly of a unit because of the separable inner or outer ring.

Ball bearings, because of the small ball contact area, must be larger than a roller bearing to give an equivalent fatigue life; however, they can withstand heavy thrust loads and greater misalignment. By using a suitable axial preload, a ball bearing unit can be made axially and radially rigid. Various materials and designs can be used for the ball separator.

The outer races of the bearings are enclosed in resilient mounts. This permits the bearing to oscillate slightly as the rotor mass spins on its gravimetric axis, thereby appreciably reducing the bearing loading caused by very slight inherent rotor imbalance or raceway eccentricity. This method is used on much of the equipment built by Airesearch, including the energy storage flywheels for the R-32 and the ACT-1 railcars.

To reduce oil windage losses in the rotor bearings, the bearings are cooled by passing oil under the inner races of the bearings through grooves cut in the shaft. The oil is jetted into the end of the shaft and thrown



out by centrifugal force through radial holes to a circumferential groove under the bearing inner race. The oil then is passed along axial grooves under the bearing race, thus cooling the inner race. There are slots in the nut (or other part adjacent to the inner race) to allow this oil to be thrown violently outward, where it contacts adjacent structures that spray the oil in fine droplets in all directions. Some of these droplets are carried into the bearings and provide lubrication. Since this is only a very small amount, the windage losses caused by oil in the outer raceway groove are reduced to a minimum. Through this system, a large amount of oil is provided for bearing cooling, but only a small amount is provided for lubrication. This matches the actual bearing requirement.

Bearing lubrication serves two functions in a high-speed operation; it provides a heat transfer medium, and it, of course, lubricates the bearing. The pressure of a lubricant itself, however, is no guarantee that lubrication will occur. The lubricant should form a full uninterrupted film between the rolling element and raceway at the operating temperature. Oils manufactured to MIL-L-23699 have excellent chemical and viscosity properties and can be used in the flywheel module.

### Seals

The shaft seal considered for the flywheel is of conventional design, typical of many applications used for high-speed machinery. The seal is a radial type with a hardened-surface steel rotor that runs adjacent to the face. A surface velocity of 285 ft/sec maximum is well within the operating regime of this type of seal. An operating life of greater than 10,000 hr is expected for this seal. Seals of this type have been developed to operate

at rubbing speeds of 400 ft/sec, 100 F, and differential pressures of 35 psig. The proper design of the seal will minimize friction losses during operation.

Figure 21 shows a typical rotor seal design which was used on the ACT-1 flywheel. The same seal design, reduced in diameter, can be considered for the flywheel module.

The selection of a radial gap seal is well suited for this application since this type of seal requires a very light contact force to provide effective sealing. The light contact force minimizes the seal friction losses and also provides a long life capability for the seal.

#### Lubrication and Vacuum Pump

A combination lube and vacuum pump similar to that developed for the University of Wisconsin Automotive Flywheel is suitable. The pump element is a gerotor (internal gear set).

The pump removes both gas and lube oil from the rotor housing. The lubrication system uses atmospheric pressure to force oil to the bearings. A molecular pump is used to aid the gerotor pump in reducing the rotor cavity to the 5 micron pressure level.



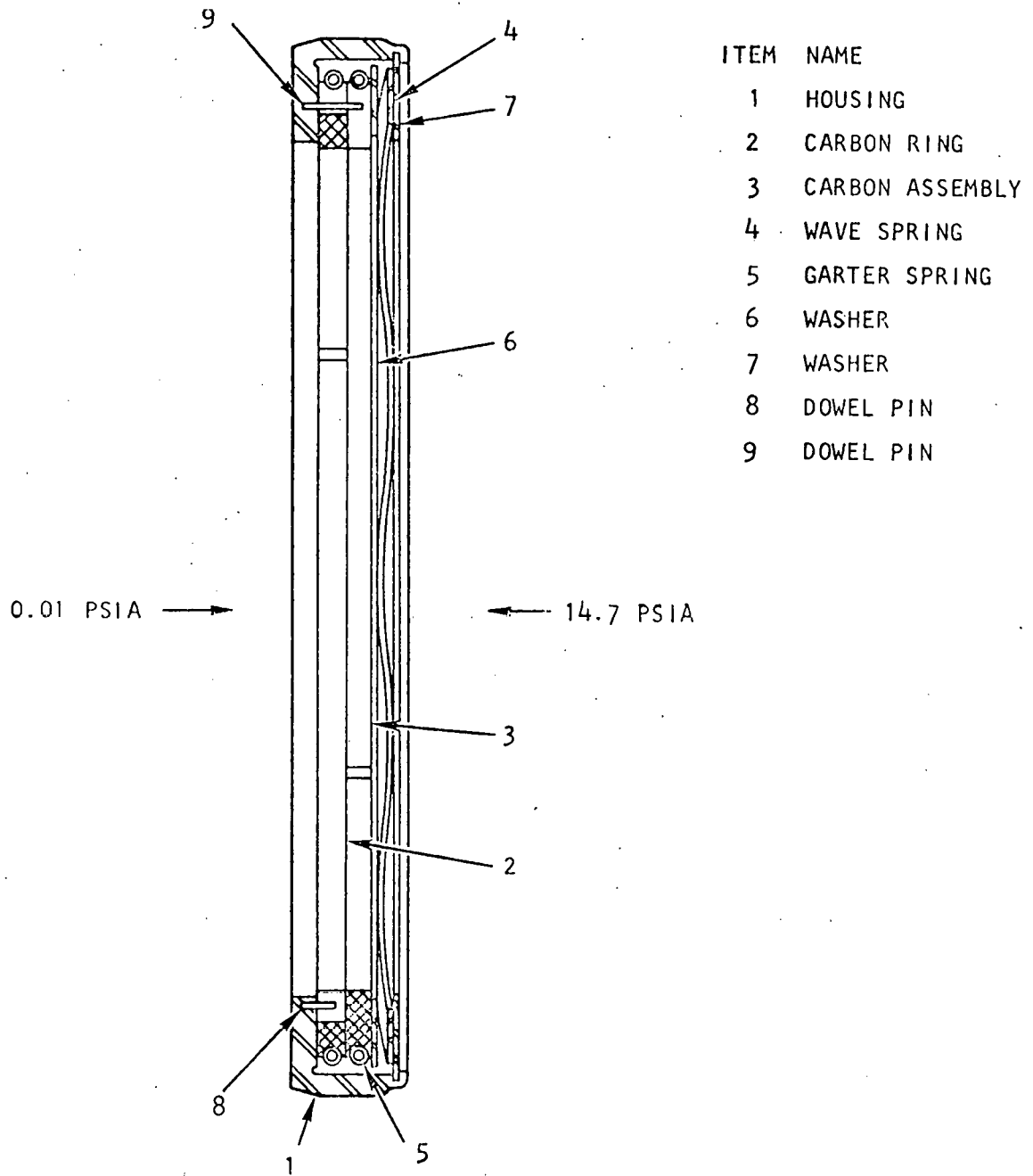


Figure 21 Typical rotor seal design

### C. FLYWHEEL SAFETY

The flywheel rotor contains a large amount of kinetic energy which is stored in a relatively small volume. The proper design of the flywheel system will allow the kinetic energy to be safely contained within the small volume under virtually all conceivable failure modes.

#### Safety Criteria

In view of the large energies being stored, it is necessary to use conservative, achievable, low-risk design practices in the flywheel design.

The safety criteria used in the design should demand:

- Conservative design stress levels, which insure that no rotor failure occurs.
- Identification of the most severe types of possible failure and analyzing their potential hazard
- Containment of the rotor for any type of rotor failure, bearing failure, or accidental vehicle impact
- Elaborate inspection and test techniques to insure proper material and fabrication quality
- Safety devices to prevent unsafe operation

#### Failure Modes

The primary, secondary and induced failure modes of a flywheel installed in a vehicle have been examined. The types and effects of the major failure modes can be summarized as follows:

<u>Likelihood</u>	<u>Failure</u>	<u>Effect</u>
Most likely	Accessory, minor component failure	Flywheel must be shut down and repaired
Likely	Accidental vehicle impact	Damage to rotating parts, possible bearing failure or rotor burst
Least likely	Seal failure	Flywheel shut down; unlikely secondary effect is explosion or fire
Extremely Unlikely	Rotor burst	Severe damage; rotor contained; no vehicle damage
Extremely Remote	Rotor burst, containment fails	Extreme danger to vehicle and surroundings; fatality possible

It is essential, therefore, to design for (1) containment in the event of bearing failure or rotor burst, and (2) preclusion of air-oil fires.

#### Rotor Burst Containment

Since uncontained rotor burst is a failure mode which could result in fatality, the flywheel design must preclude bursts during normal operation. Proper selection of operating stress levels, environmental conditions, and inspection procedures will preclude a burst failure during the design life (number of operating cycles) of the rotor. Containment will then be provided to prevent fatalities. For a composite material rotor, containment material is selected for hydrodynamic burst. Material volume is based upon the total translation of kinetic elements. The containment ring housing is free to rotate so that any momentum transferred goes into spinning the ring rather than breaking the flywheel loose from the vehicle. The containment and casing structure will also provide sufficient mass to absorb the heat generated in the event of a rotor rub.

### Bearing Failure Containment

The most likely major damage failure mode would be a bearing failure. This can occur from a lack of lubrication, bad bearing material, or severe loads caused by an accidental impact. The shaft supporting the flywheel and the surrounding casing can be designed so that in the event of a failure, the shaft and its shoulder will rub on a bumper on the casing and prevent the flywheel itself from rubbing on the casing. In this manner, the flywheel will be contained until it can be decelerated.

### Inspection

To insure the safety and reliability of the flywheel, rigorous inspection procedures should be followed. These procedures are similar to those listed below:

They include:

- Checks on composite and motor material strength by material sampling.
- Ultrasonic and magnetic particle inspection of metallic parts.
- Whirl test of rotor at overspeed.

Of these, ultrasonic and magnetic particle inspections determine the homogeneity of the metallic material, while the material sample test and overspeed whirl pit test insure proper material strength.

### Safety Devices

Safety devices necessary for the design include:

- Two Overspeed Trips -- One trip is electronic and is initiated by the flywheel RPM transducer, the other trip is mechanical and operates due to centrifugal force generated as the speed increases.
- Low Oil Pressure Trip -- Insures the bearings are never starved for oil.

### Preventive Maintenance

Periodic maintenance can be scheduled to insure the fewest possible failures. The major inspections or replacement and probable time between inspections are listed below:

<u>Item</u>	<u>Operation</u>	<u>Period</u>
Seals	Replace	5 years
Bearings	Replace	5 years

### Major Failure Acceptability

There is always the possibility that an uncontained failure could occur because of a completely unforeseen sequence of failure modes, severe accidental impact damaging the containment shield, some combination of material failure, or human failure. This should not preclude the use of flywheels in vehicles, however, since some risk is acceptable if resulting benefits to the population as a whole are high. Calculation of the costs or benefits is difficult, but they seem to follow a sigmoid curve, reaching a point where it simply costs too much to reduce the fatality rate, or where the risk is sufficiently low. As an example, containment is not provided for a tri-hub burst on commercial jet aircraft engines because the additional weight would reduce the plane's carrying capacity and result in an increased cost in conveyance.

## SECTION II POWER TRANSMISSION DESIGN

### A. ELECTROMECHANICAL TRANSMISSION

The crux of the power transmission problem is to efficiently couple a decelerating flywheel to an accelerating vehicle and, conversely, an accelerating flywheel to a decelerating vehicle. The transmission method must also translate high unidirectional flywheel rotor rotational speeds into lower forward and reverse axle speeds. In addition, the speed of the traction drive motor, when battery connected, should be high enough to prevent an excessive current drain on the battery. Normally, an electric motor presents a low resistance path to the battery until the speed is high enough to generate a substantial back EMF.

Three power transmission configurations are shown in Figure 22:

- Hydromechanical
- Pure Electrical
- Electromechanical

The electromechanical transmission has been selected as being the most efficient, lowest cost, most reliable and of similar weight to the hydromechanical and purely electrical transmission. This transmission concept utilizes a mechanical transmission and two motor/generators.

#### Mechanical Transmission

One means to accomplish the required speed conversions is the planetary (epicyclic) gear set, which has been chosen for this application. An artist's conception of a planetary gear set is shown in Figure 23. As can be seen from the Figure, unidirectional drive input torque is reacted by two output drive torques, hence the name: Split Drive. The planet gears, free to rotate on studs attached to the carrier, are interposed between the sun and ring gears.

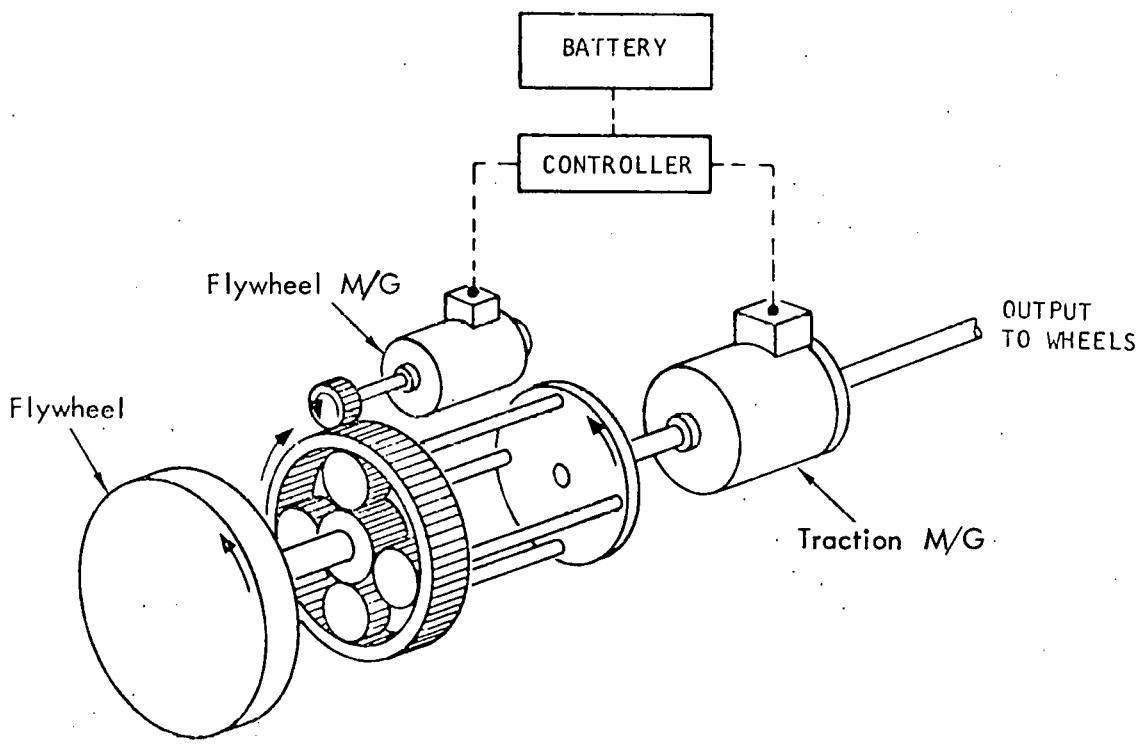
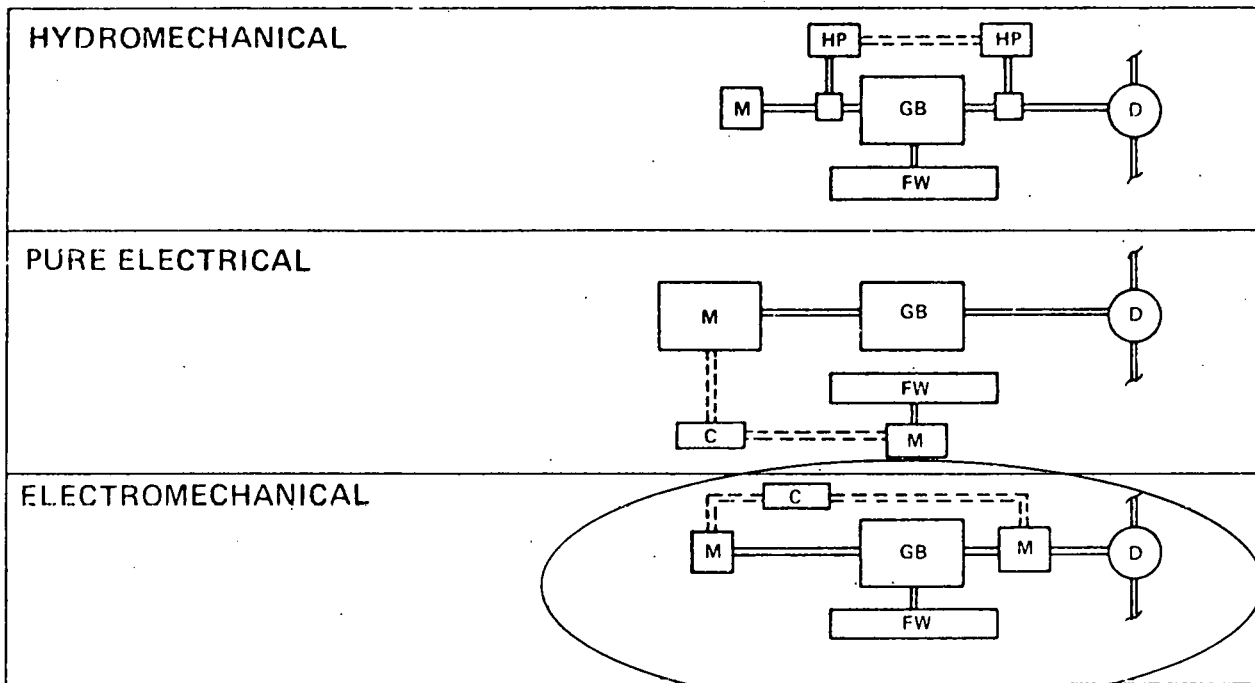


Figure 22 Power transmissions

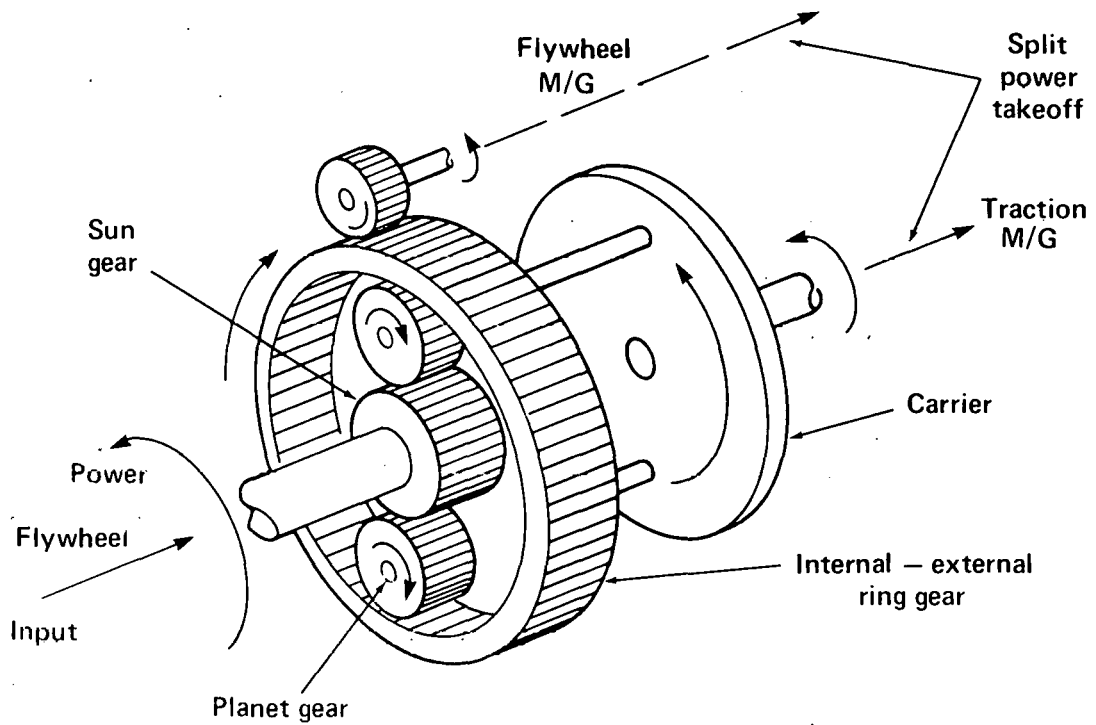


Fig. 23 The split drive concept: a variable speed transmission.



Hence, they divide the input torque, adjusting to the two output drive torque demands. Note that the sum of the two demands is always equal to the input torque less friction losses. Any ratio of demands is acceptable. Either or both drives can reverse. Thus, the split drive concept provides a stepless, variable speed, reversible transmission.

The principle of power transmission utilizing the planetary gear set is described in Figure 24. When the vehicle is at rest and the traction motor is stationary the sun gear and flywheel turns at high speed (40,000 RPM) while the flywheel M/G is coupled to the ring gear which turns at 5,000 RPM. When it is required to start the vehicle, the electrical output of the flywheel M/G operating as a generator, is connected to the traction motor. The torque for the initial acceleration of the vehicle is drawn from the flywheel with the battery supplying control power only.

Referring to the plot of Vehicle Speed vs. RPM in Figure 24, energy is extracted from the flywheel to accelerate the vehicle from rest to 55 miles per hour. This decreases flywheel RPM to approximately 36000. Flywheel generator RPM also decreases as shown during the acceleration. Flywheel energy is supplied as drive power to the traction motor, accelerating it to approximately 6000 RPM and hence, the vehicle to 55 miles per hour.

When a grade is encountered, energy is supplied by the flywheel to augment the battery demand. Battery power demand is thus stabilized. Dependent upon the severity of the grade, flywheel RPM may drop to 20,000 as shown by the "grade load" line on Figure 24. Flywheel generator and traction motor RPM will also decrease as shown with the vehicle velocity decreasing to 50 miles per hour.

Approximately half the torque output of the flywheel is transmitted electrically through the flywheel motor to the traction drive motor. The other half of the torque output of the flywheel is transmitted mechanically through the planetary

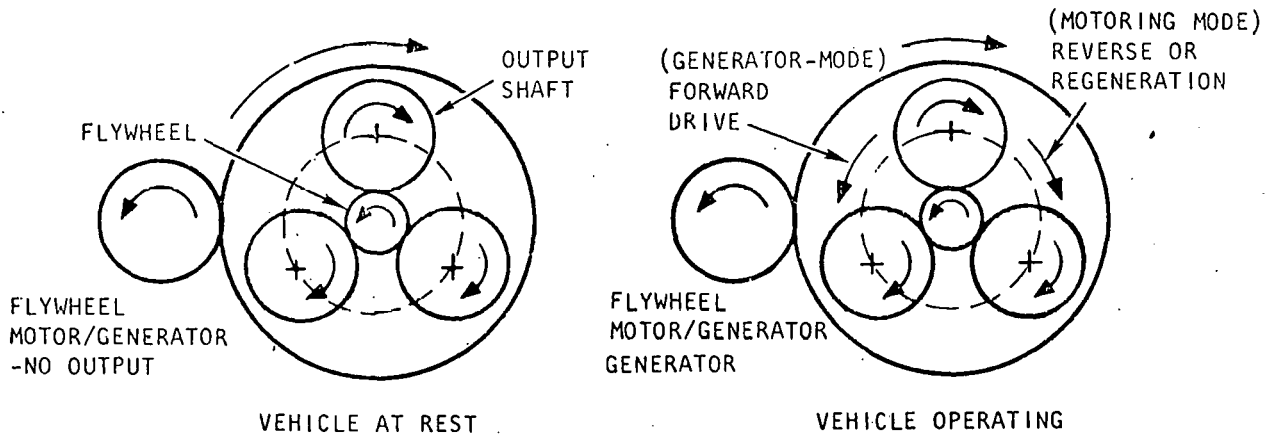
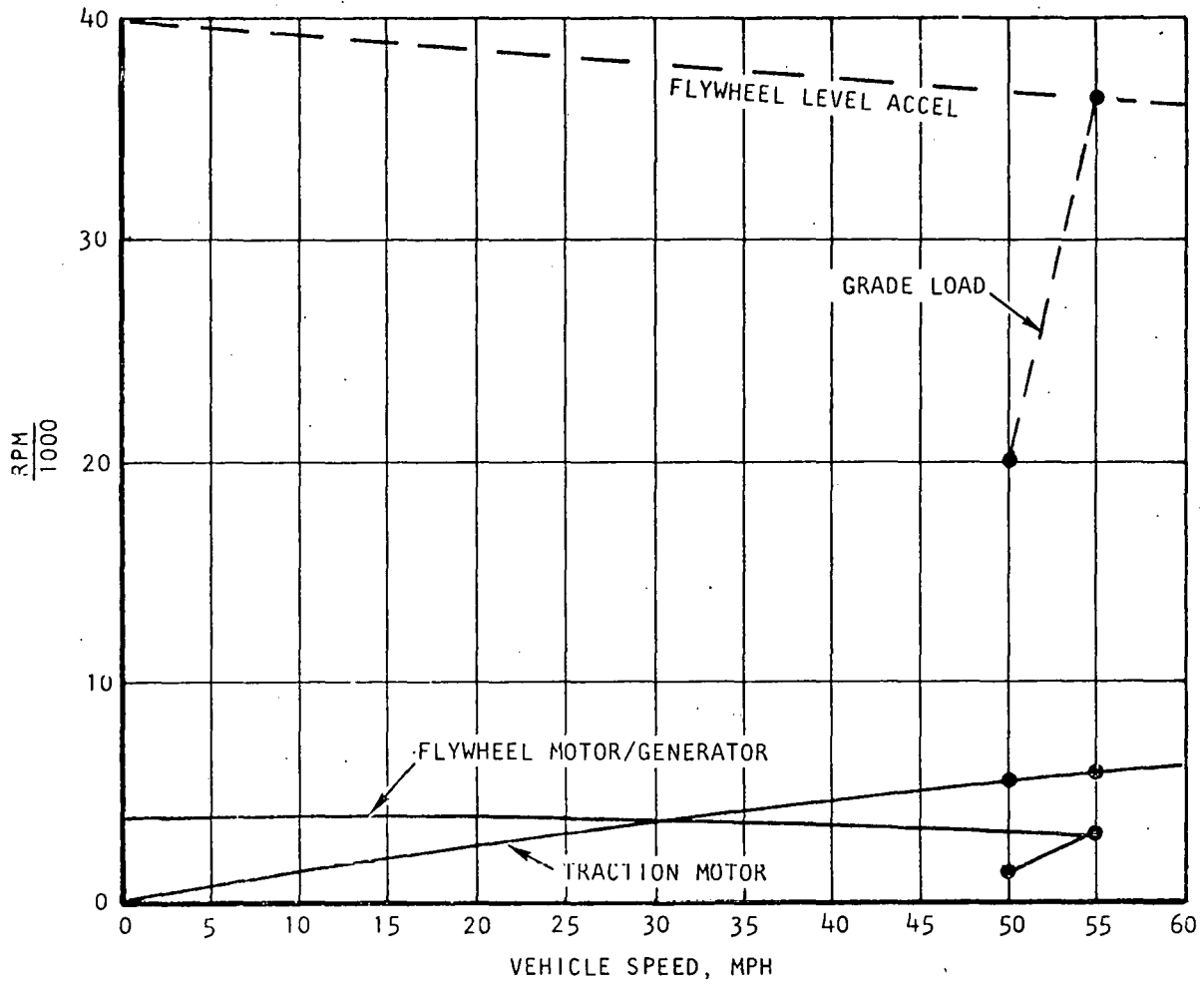


Figure 24. Principle of power transmission

drive train. The relative speed of the flywheel to the traction drive motor can therefore be varied steplessly from reverse through zero to full forward speed by proper control of the ring speed via the flywheel motor.

The above principle of speed control has been used by Airesearch previously on the cabin air compressor for the Super Constellation except that the torque link was hydromechanical rather than electromechanical.

Figure 25 shows two views of the planetary gear system as described above. This planetary system weighs approximately 10 lbs and transmits 100 hp in the same speed range as described.

#### B. TRACTION MOTOR AND FLYWHEEL MOTOR

The DC motors selected for flywheel and traction drive are separately excited machines developed by Airesearch. The motors are designed for the operating modes described previously and to be compatible with the power and control circuits of the power system. The special features are fully compensating pole-face winding, separate excitation, and laminated frame. Typical motor generator performance is shown in Figure 26. Figure 26 portrays a separately excited machine with a lower maximum RPM capability. The parameter relationships shown are valid for the higher speed machines planned for this application.

The armature consists of laminations, fabricated of electrical grade steel M36, which are insulated from each other. The slots are rectangular and are closed with high-temperature, high-strength, fiberglass slot wedges. The commutator is of the ring nut-type construction and is tested at an over-speed of 120%. The armature coils are made from rectangular copper wire, insulated with polyamide file (Kapton) which is fused to the copper and to itself. The ground insulation consists of a Kapton wrapper. Glass-tape is used as a binder and resin carrier to give the coil abrasion resistance. The whole armature, up



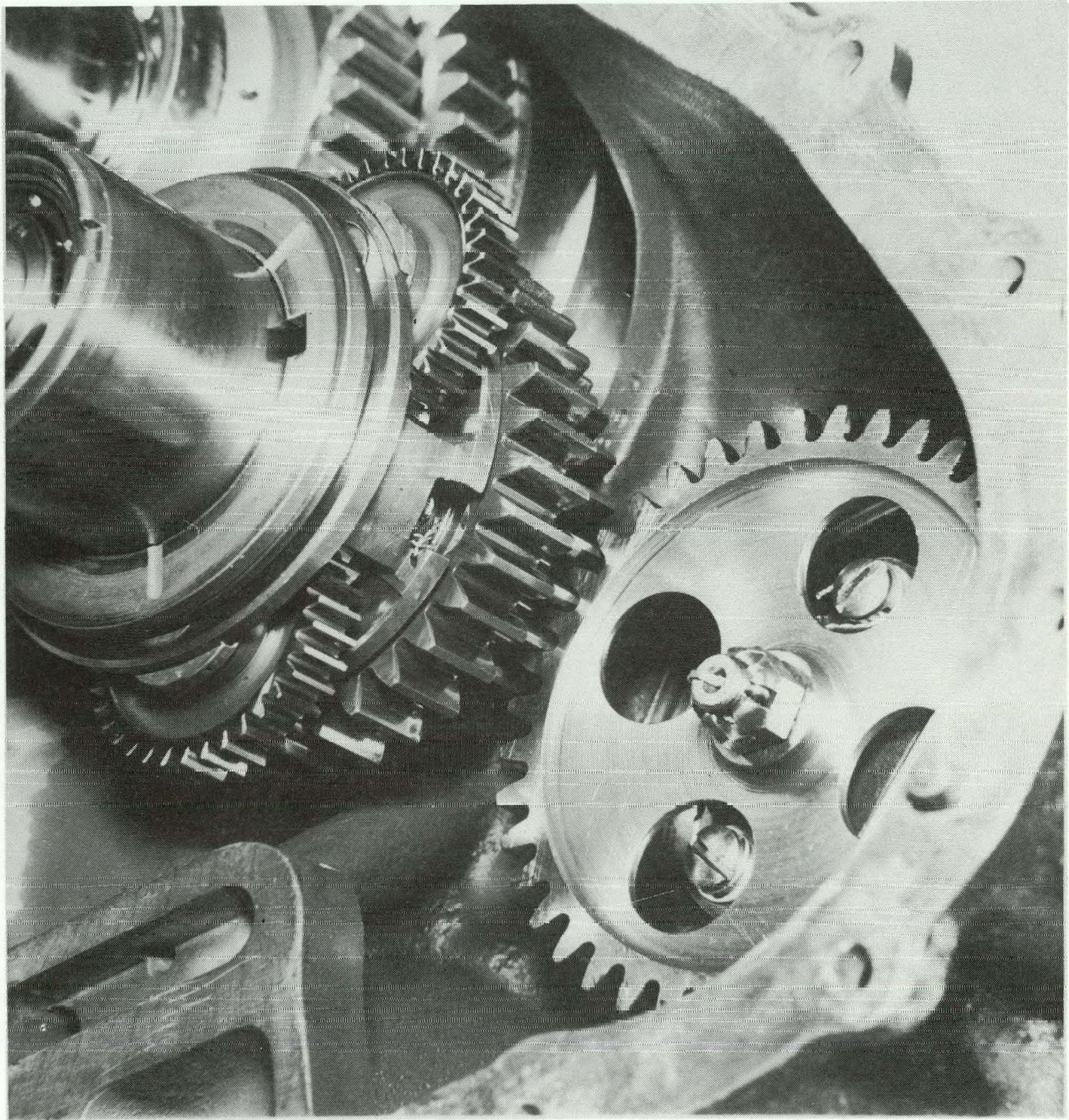


Figure 25A. Typical Airesearch cabin air compressor epicyclic transmission, 100 hp



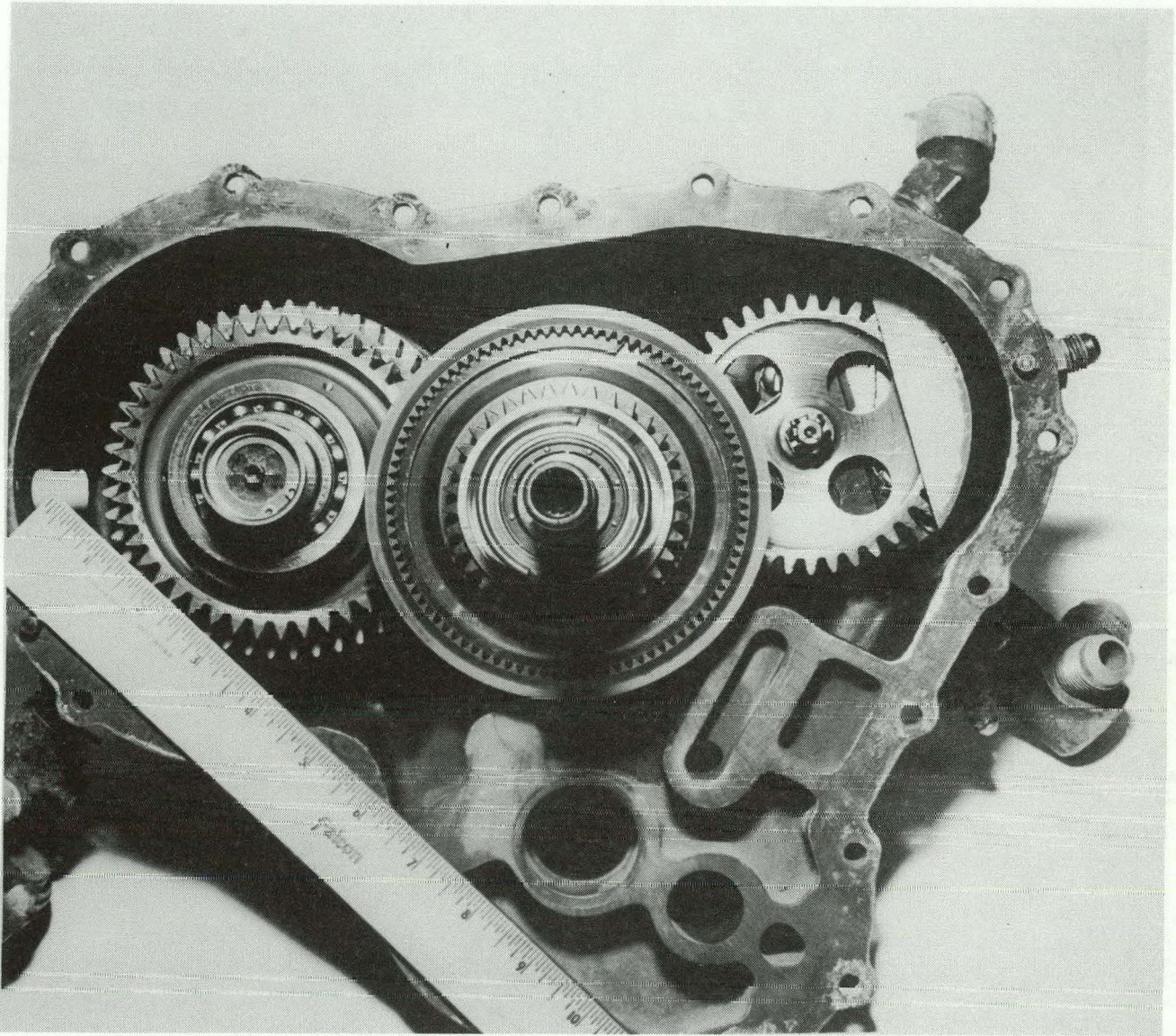


Figure 25B. Typical Airesearch cabin air compressor epicyclic transmission, 100 hp

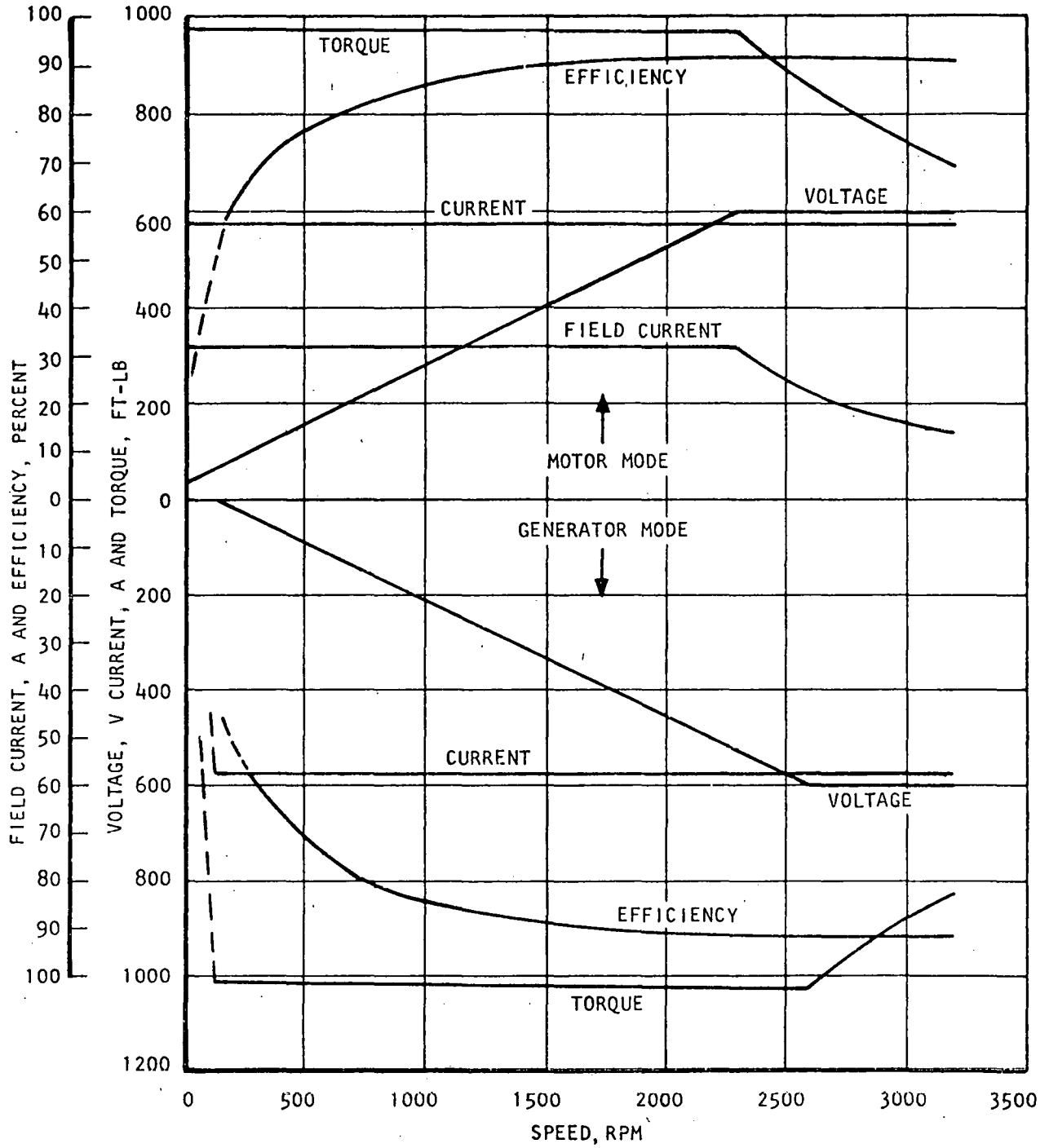


Figure 26 Typical motor generator performance

to the commutator risers, is vacuum-pressure impregnated in solventless silicone resin and is then partially oven cured.

The armature shaft has an extension with a cylindrical fit to mount the coupling. The shaft is held in axial position by a ball bearing at the commutator end. The roller bearing on the other end has an inner ring with down-tapered ends to allow free floating action. The grease cavity is sealed on the ball bearing by a long shaft sleeve, and on the roller bearing by piston ring seals that allow very small labyrinth clearances without having rubbing surfaces.

The magnetic portion of the stator frame consists of laminations made from electrical grade steel M36 that are insulated from each other. The four main and four interpole laminations are made from the same steel. The poles are held together with rivets; on the interpoles, the rivets and rivet-heads are insulated from the polestack. Individual coils can then be exchanged without disturbing others. The motor is separately excited. The brush rigging consists of steel bars and press-plates that are precision-drilled to locate the brush holder insulation studs and ensure accurate lineup of poles and brushes. Each of the four brush holders has two split brushes with stranded copper shunts. The brushes have resilient fiberglass-topped pads to distribute the spring pressure and to dampen vibrations.

The stator is of welded construction. A stack of frame laminations is pre-loaded and then held together by end rings with eight bars welded to the rings, one of which is integral with the cast steel bell housing. The whole construction offers a stiff and lightweight frame. The drive end-bell is made of nodular iron which supports the bearing. The brush access holes are covered with quick-release covers, one of which supports the air inlet.

SECTION III  
CONTROL SYSTEM DESIGN

A. COMPONENT DESCRIPTION

The control system required for the hybrid propulsion system is shown in Figure 27.

The electronics design can incorporate current "state of the art" digital techniques with solid state conversion devices utilized for interfacing.

The proposed design does not utilize high power solid state devices in the motor armature circuits, thereby eliminating the losses normally associated with control elements such as "choppers".

The major components which make up the control system are the Power Control Unit (PUC) and the "on board" battery charger.

Power Control Unit (PCU)

As seen in Figure 27, the PCU contains the microprocessor, instrument and control interfaces, armature and field control and the necessary power supplies

a) Microprocessor ( $\mu$ P). The heart of the PCU is the PROM (Programmable Read Only Memory) programmed microprocessor through which all auto control commands are executed. The PROM can be preprogrammed to implement the desired control algorithm, and can be reprogrammed if necessary for optimization during vehicle checkout. Temporary, continuously updated storage of current operational status; i.e., flywheel RPM, road speed, battery charge level, operator command, etc., can be in registers and RAM (Random Access Memory).



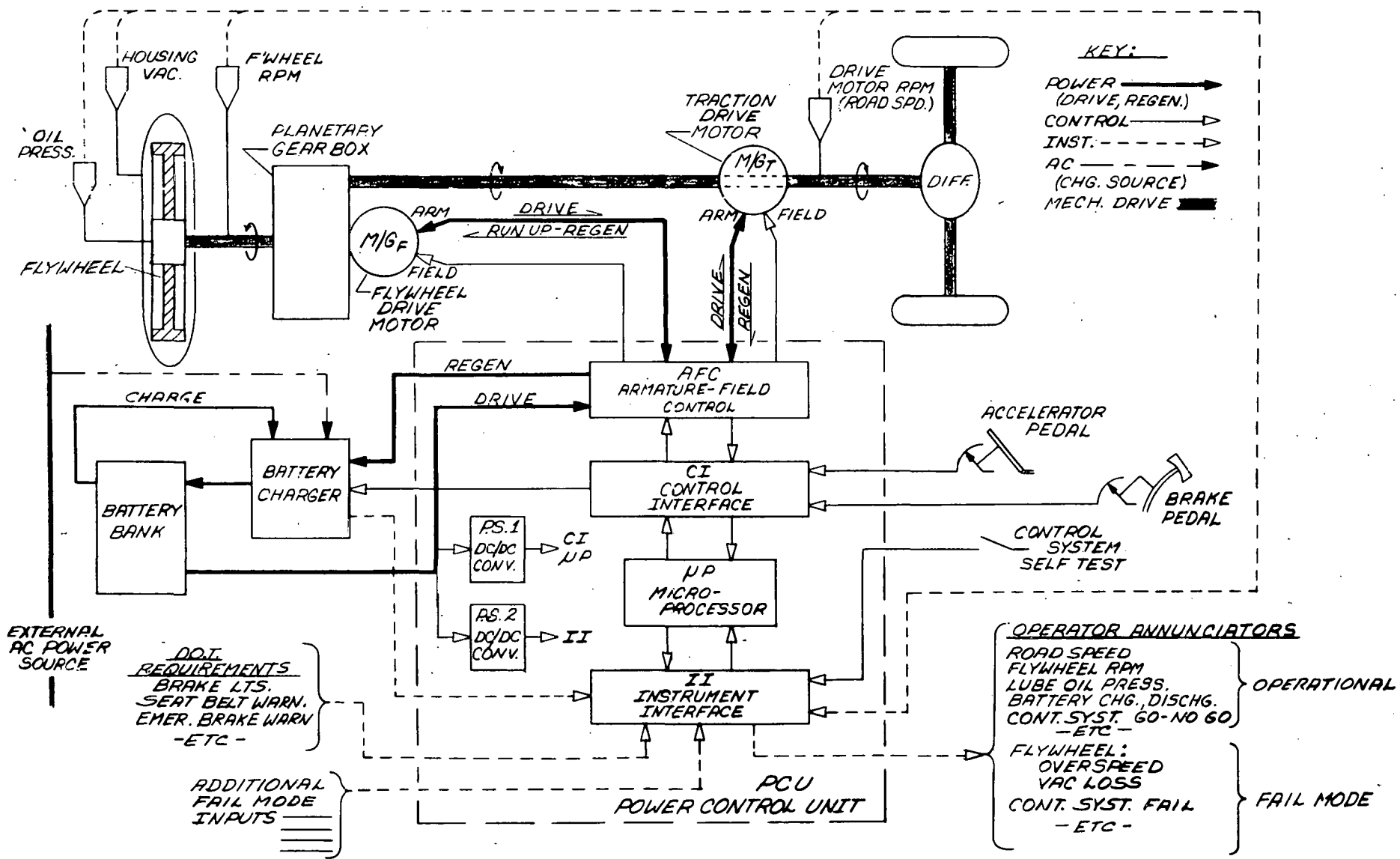


Fig. 27. Propulsion control system.

The MSC-80 microcomputer system developed here at LLL can be utilized. The MSC-80 design incorporates Intel Corporation's 8080 Central Processor.

The 8080 is an 8 bit parallel central processing unit for general purpose digital computer systems. It is fabricated on a single LSI (Large Scale Integration) chip using Intel's N-Channel Silicon Gate MOS (Metal Oxide Semiconductor) process.<sup>17</sup>

LLL has designed, fabricated and currently stocks loaded printed circuit boards for the MSC-80 system.

Software simulators and assemblers are currently running on the LLL "Octopus" computer system.

The capability of programming, erasing and reprogramming the PROM memory exists in-house at LLL.

b) Control Interface (CI). The CI will contain the electronics required to convert a  $\mu p$  digital command to the voltage/current levels necessary for system control. Analog to digital conversion of operator commands such as speed and braking demand would also be accomplished in the CI, with the resultant digital input fed to the Microprocessor.

Microprocessor commands to the Armature/Field Control (AFC) will be conditioned by the CI to provide the voltage and current levels required as control inputs.

Commands to the battery charger determining charge rate initiated will be conditioned by the CI. These commands will be based upon current battery "state of charge" as monitored by the microprocessor through the Instrument Interface.

c) Instrument Interface (II). A separate stand along interface II with accompanying power supply is utilized for all operational parameters monitored as well as fail mode inputs. Electronically divorcing the II from the Control Interface and the Microprocessor will aid in assuring operator alert of any fail mode condition in the event of control system ( $\mu$ p, CI) failure.

Operational parameters and fail mode functions are supplied as command inputs to the  $\mu$ p and to the operator's indicator panel. Panel indication may be digital, analog, or auditory.

At start-up, control system self test is automatically initiated through the II which commands the  $\mu$ p to run a control system diagnostic routine with the go - no go result displayed for the operator.

The II will also interface to all general housekeeping demands such as Department of Transportation requirements; i.e., brake lights, seat belt and emergency brake warning, key warning (inserted in ON-OFF switch), etc.

d) Power Supplies (PS 1, PS 2). The control system power supplies will convert battery bank DC voltage to the levels required by  $\mu$ p, CI and II digital logic and interface circuitry.

PS 1 will supply the  $\mu$ p and the CI while PS 2 provides power for the II.

e) Armature/Field Control (AFC). The Armature control portion of the AFC will house the starting resistor and contractor armature switching circuitry as shown in Figure 28. Switching commanded by the  $\mu$ p through the CI will pick up and drop the flywheel M/G starting resistors and connect motor generator armatures when one machine is generating and the other motoring.

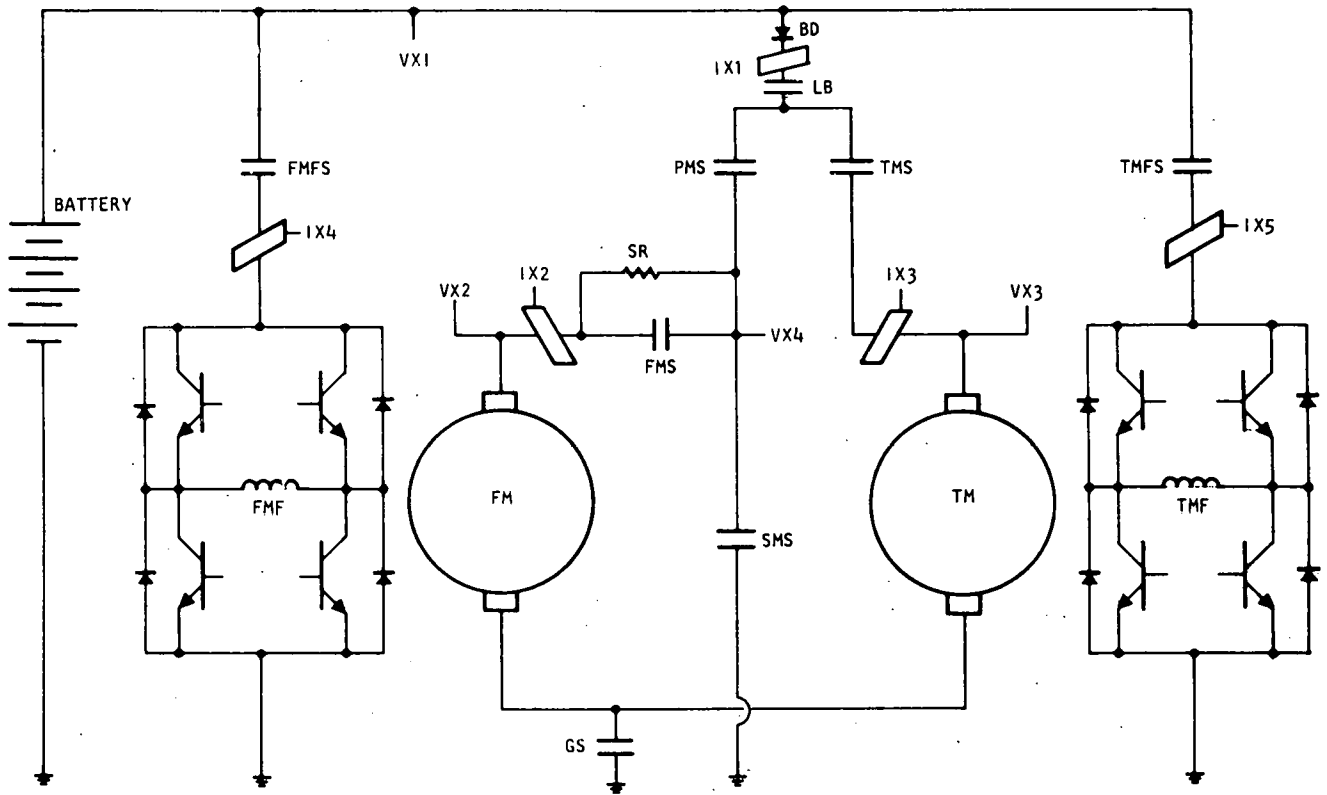


Figure 28 Armature and field control

The starting resistor is a stack constructed of nickel-chromium wire sized for the current carried. The stack can be cooled by under hood air.

The field excitation supplies with output level and polarity-controlled by the  $\mu$ p through the CI will also be housed in the AFC. Differential pulse width modulation will be utilized for field control.

### Battery Charger

Lead-acid batteries should be charged for a sufficient length of time, and at such a rate as to introduce into the battery the ampere-hours discharged, plus a 5 to 15 percent overcharge. Any charge rate is permissible which does not produce excessive gassing or a cell temperature greater than 115°F (46.1°C).<sup>7</sup>

Figure 29 shows that a discharged battery can absorb high currents at a relatively low voltage. As the charge progresses at a given rate, the voltage increases with the higher charge rates yielding higher voltages.

For the Hybrid Commuter application, overnight charging will be by the Taper method based upon an eight hour charge time for a fully discharged cell. Figure 30 shows the typical voltage, current and specific gravity profile of a cell being charged by this method.

The circuitry of the charger is such that initial and finish charge rates are matched to the battery. The initial charge rate used is approximately 20 amperes per 100 ampere hours of battery capacity (C/5 rate). The finishing rate is to be C/20 or 5 amperes per 100 AH capacity.

Overnight charging (8 hours) will draw upon a public utility power source. Vehicle motor generators can serve as the charging power source under the following operational conditions:

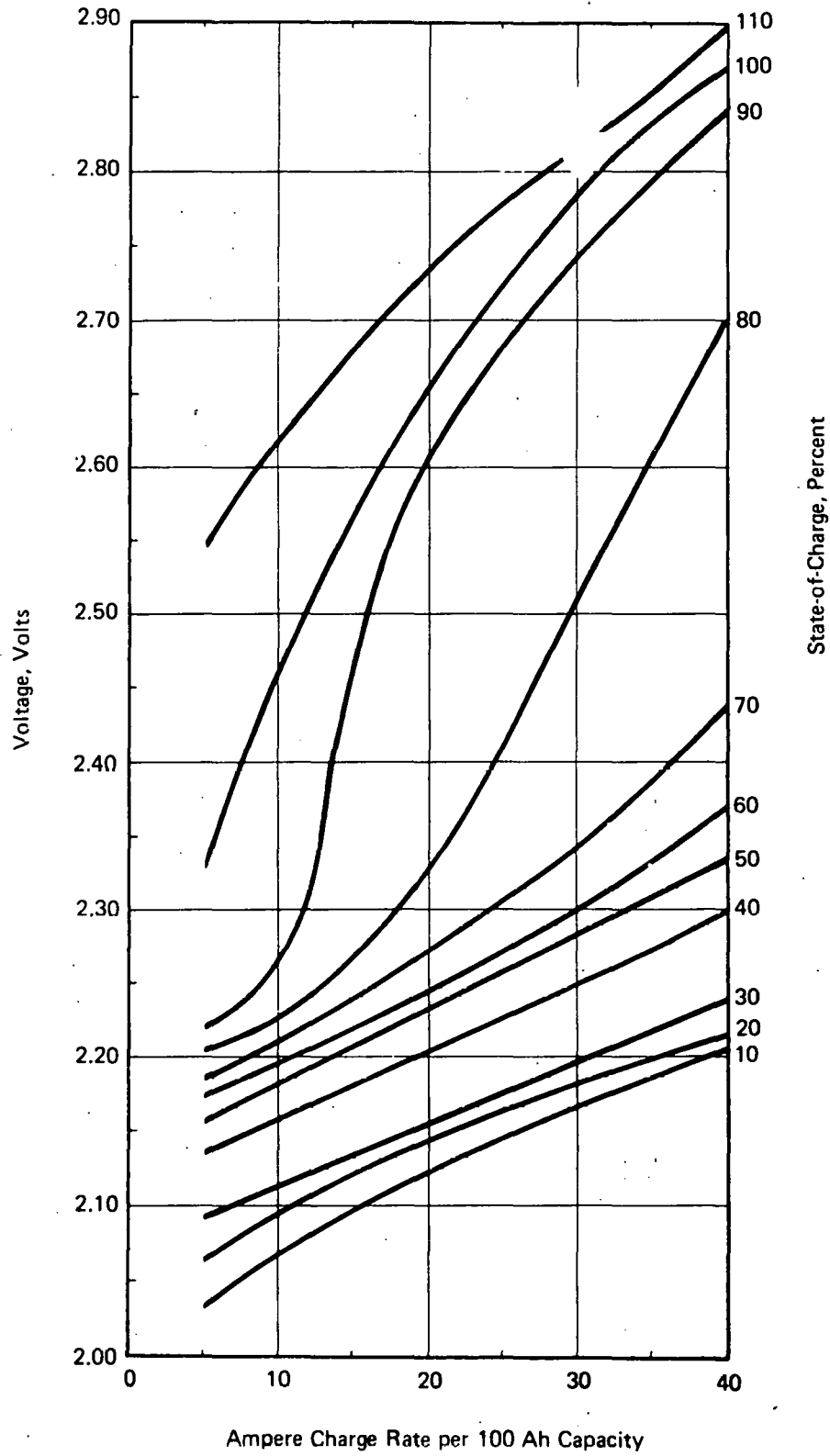


Figure 29 Lead-acid charging voltage per cell vs charging rate at various states-of-charge

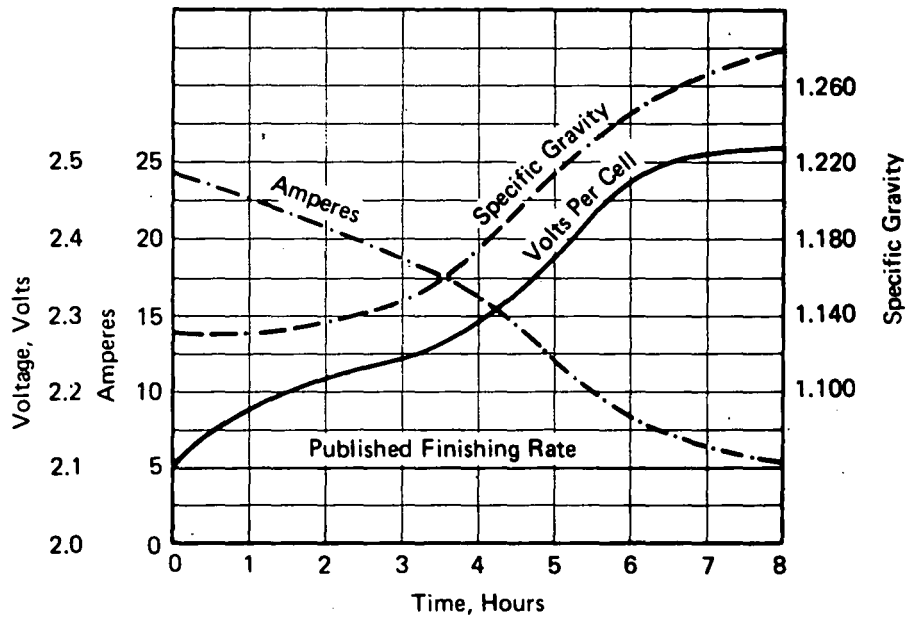


Figure 30 Lead-acid charging typical taper charge profile for 100 Ah cell

a) Prolonged Parking. Total flywheel energy loss through run-down when parking for an extended period can be averted if energy transfer via the flywheel generator to the battery bank is initiated by the operator.

b) Regenerative Braking. On an extended down-grade, following flywheel run-up to maximum RPM (start point of Figure 10). Limited regeneration to the battery might be possible. As stated in Volume 1, Section Five-D, this should be investigated.

The charge rate initiated, under the above conditions, will be that required to match the battery state of charge as determined by constant monitoring of battery charge level (Reference Figure 30).

#### B. OPERATIONAL MODE CONTROL

The flywheel and traction motor/generators will be utilized in either a motoring or a generating mode depending on the control requirement. To aid in explanation of operation, the machines will be referred to as a motor or a generator to reflect the current mode of operation.

#### Operational Description

For the commuter mode of operation, flywheel and battery charging will draw upon public utilities power and be accomplished overnight (8 hour period). Battery charging will be by the 8 hour Taper method with a flywheel run-up timer initiated approximately 30 minutes prior to expected departure. Minimum flywheel run-up time from zero to maximum RPM is approximately 15 minutes.



a) Flywheel charging. During initial winding of the flywheel with the vehicle at rest, the vehicle brakes should be applied. Upon initiation, a starting resistor limits the maximum current supplied by the battery to the flywheel motor until base speed is attained and the resistor is bypassed. The flywheel is accelerated until RPM reaches the maximum level as shown by the start point in Figure 10.

Following initial flywheel run-up to the maximum operating level, outputs from speed sensors monitoring traction drive motor RPM (road speed) and flywheel RPM, are utilized by the Power Control Unit to hold flywheel RPM within the control band of Figure 10. The kinetic energy of the vehicle plus the kinetic energy of the flywheel is maintained constant thereby providing the energy base required to meet acceleration demand with a margin for RPM increase adequate to accept energy during deceleration.

The AFC switch sequencing and field strength variation commanded by the  $\mu$ p for the flywheel charging is as follows: (Refer to Figure 28)

- Close flywheel motor field switch (FMFS) excite the field of the flywheel motor at approximately its full field value.
- Close ground switch (GS), parallel motor switch (PMS), and line breaker (LB). The armature of the flywheel motor and the starting resistor (SR) are now in series across the battery, causing the flywheel motor to accelerate.
- When the flywheel is close to its equilibrium speed and the current flowing in the motor armature has dropped to a low value, the flywheel motor switch (FMS) is closed, cutting out resistor SR and putting the motor armature across the line.
- The acceleration of the flywheel now continues by field weakening the motor. When the flywheel has reached operating speed, the starting sequence is complete, and can be left idling if necessary.

b) Vehicle Operation. To initiate reversal motion with the flywheel charged, the operator selects reverse, releases the parking brake, and depresses the accelerator. In response to the operator commands, field weakening of the flywheel motor is initiated. Motor RPM increases tend to increase flywheel RPM. With the planetary carrier free to rotate (brakes released), flywheel reaction against an increase in RPM is translated to the planetary carrier. The carrier rotates in the reverse direction resulting in reverse vehicle motion. Vehicle reversing power is supplied by the flywheel with vehicle velocity limited at 10 miles/hour.

To initiate forward motion the operator selects forward, depresses the accelerator pedal reversing the shunt field and connecting the armature of the flywheel motor to the traction motor armature. The flywheel motor then operates as a generator to drive the traction motor using energy supplied by the flywheel. Additional torque is also transmitted mechanically directly through the planetary arm of the transmission. Rate of acceleration is controlled by the accelerator pedal position input to the Power Control Unit which in turn controls the strength of the generator field. Energy is thus supplied by the flywheel during acceleration with the battery supplying control power only.

The AFC switch sequencing and field strength variation for operation during acceleration is as follows:

With the flywheel at operating RPM and switches GS, FMS, PMS, and LB closed, the vehicle is ready to move. The sequence is:

- Increase the field of the flywheel generator slightly so that the generated voltage is higher than the line voltage. The input rectifier diode (BD) blocks, making the line current zero.
- Open line breaker LB.
- Reduce the field of the generator to zero.

- Close traction motor switch TMS.
- Apply full field value to the traction motor field (TMF) by closing switch TMFS.
- Release the parking brakes.
- Slowly increase the field of the flywheel generator, which circulates its armature current into the traction motor generating a back EMF, which is overcome by further increasing the field of the flywheel generator. This mode of acceleration continues with the traction motor current, sensed by the current transducer IX3, controlled at the commanded value by the flywheel field supply. The traction field supply will remain at maximum.
- This mode of acceleration comes to an end at base speed, which is when voltage sensed by VX2 and VX3 is slightly higher than that sensed by VX1.

Base Speed Transition: When the traction system voltage as sensed by transducers VX2 and VX3 is slightly higher than the battery voltage VX1, base speed transition is initiated as follows:

- Close the line breaker LB. No current flows since VX2, VX3 is greater than VX1 and input diode BD is back-biased.
- Slowly reduce the traction system voltage VX2, and VX3 by reducing the field current to the traction motor and the flywheel generator. When this voltage equals the battery voltage, current will flow from the battery into the flywheel and traction motors. Both M/G's are now in a motoring mode. The control of the magnitude of the current in each of these two parallel paths as sensed by IX2 and IX3 is transferred to the respective field supplies. This completes the base speed transition.

Upon receipt of a decreased acceleration demand from the operator, the PCU commands the transfer of traction motor power source from flywheel to battery. With acceleration demand and vehicle velocity constant, the battery provides drive motor power plus the power required by the flywheel motor to replenish flywheel run-down losses.

When the line breaker LB is closed, the voltage across the traction system is the battery voltage. The current in the traction motor is controlled at the commanded value by the traction motor field supply.

The flywheel is now placed on a speed schedule that is a function of vehicle speed. This speed schedule is maintained by flywheel field supply variations commanded by the  $\mu P$ , based upon speed sensor inputs.

The flywheel speed schedule calls for lower flywheel speeds at higher vehicle speeds, thus ensuring an adequate RPM margin for the kinetic energy of the vehicle. The operator can call for braking at any instant of time and the flywheel will not be flooded on a level roadway. The flywheel supplies power to the vehicle as long as it continues to accelerate. The power demand on the battery is thus stabilized.

When an up-grade is encountered the current demand on the battery increases in an effort to maintain commanded velocity. When battery current exceeds a preset limit, flywheel energy via the flywheel generator fulfills the additional power requirement holding battery current constant. The battery current level above which flywheel augmentation will be initiated will be determined through computer simulation studies of control system performance during the development phase of the program. (Reference Section V-C).

Removal of accelerator pedal pressure by the operator signals the PCU to reverse the traction motor shunt field (changing it to a generator) and connect its armature to that of the flywheel motor. The traction generator now

supplies power to the flywheel motor to accelerate the flywheel. The degree of regenerative braking is controlled by PCU-commanded flywheel motor field strength variations based upon brake pedal position with no accelerator pedal pressure applied. With no pressure applied to accelerator or brake pedals, the degree of regenerative braking commanded will be comparable to the compression braking of an I.C. engine equipped vehicle with a standard transmission.

On long down-grades the flywheel RPM may tend to rise above the start point of Figure 10. At this point the starting resistor will be switched into the armature circuit of the flywheel motor and the excess energy dissipated.

AFC switching and field strength variations during deceleration are as follows:  
follows:

The commanded braking currents are now negative and the system responds by a slight increase in the field of the traction motor. This reverses the flow of current and raises the voltage across the traction motor, causing the input diode BD to block and the battery current to go to zero. The traction generator supplies current to the flywheel motor increasing flywheel RPM. The field supplies regulate the current in the armature(s) of the respective machines, which in turn varies the degree of braking.

Base Speed Braking Transition: This consists of opening the line breaker LB when voltage VX3 is slightly greater than the battery voltage VX1. The line breaker LB is kept closed above base speed so that a transition back to motoring would not require a reclosure of LB.

This braking mode continues until the flywheel machine field is reduced to zero. With the traction motor field at maximum, this produces a linear cushion-off of braking effort, which becomes zero at zero vehicle speed.

The friction brakes need not be applied until after the vehicle has come to a stop using the electric brakes.

Braking at High Speed: If full braking rate is commanded at high speeds, the maximum voltage capability of the flywheel motor may be exceeded. When this condition is sensed by the control system, switch FMS is opened, putting the starting resistor SR in series with the flywheel motor. This allows the traction motor voltage to go as high as needed to provide the braking effort commanded. Some of the braking kinetic energy is now dissipated. When the speed of the vehicle has dropped sufficiently, the switch FMS is closed and the excitation of the flywheel motor is adjusted in the appropriate manner.

SECTION IV  
PERFORMANCE CALCULATIONS

A. RATIONALE

This section outlines the calculations which support an initial assessment of performance of the battery-flywheel hybrid vehicle. Performance characteristics are compared with those of an all-battery electric vehicle of the same size and weight. Characteristics of interest include power and energy requirements, the vehicles' touring range under a variety of driving conditions, and grade and acceleration capabilities.

First of all, basic assumptions must be made which describe a vehicle's level road tractive resistances - rolling and air resistance. Simplified equations, which assume a constant average rolling resistance force with respect to velocity and also that air drag follows a velocity-squared relationship, were used. These simplified expressions yield results which are within the experimental variations for real vehicles of similar payload capacity. The same road-load coefficients were used for both the hybrid and the battery-electric vehicles.

In addition to steady-state operating conditions (e.g., constant 55 mph on a level road), both conceptual vehicle types were evaluated with respect to stop-and-go urban driving schedules. These schedules have been defined by the Society of Automotive Engineers for the purpose of electric vehicle testing.

Power and energy relationships were computed by dividing these driving cycles into constant-velocity and constant-acceleration segments. Energies for each segment were summed algebraically to obtain the total energy per cycle.

Some fundamental differences were assumed for the two propulsion systems:

1. The hybrid system was assumed to have a regenerative braking capability.

This takes advantage of the fact that flywheels are better able to accept

high recharge rates. The battery-electric was assumed not to be equipped for regenerative braking.

2. When batteries alone are the energy storage device, the extractable energy is strongly dependent (and limited by) the drain rate. Even a small flywheel provides substantial relief from this restraint.

Average estimated values for component efficiencies were used to determine the energy flows from and to the storage devices. An estimated run-down loss was charged to the flywheel module.

This is a preliminary evaluation. Therefore, the direct comparison of hybrid vs. electric vehicles is based on energy requirements at the output of the energy storage devices. Vehicle accessory loads, battery internal losses, battery charger losses, and system efficiencies beyond the vehicle have not been taken into account in this report.

## B. VEHICLE DESCRIPTIONS

### General Specifications

Vehicle Description: Two-passenger, special purpose urban commuter vehicle

Curb Weight	907 Kg (2000 lbs)
Payload Weight	181 Kg (400 lbs)
Test Gross Weight	1088 Kg (2400 lbs)
Power Train Weight	465 Kg (1025 lbs)
Weight of Energy Storage Devices (Included in Power Train Weight)	385 Kg (850 lbs)
Rolling Resistance Coefficient	0.012
Projected Frontal Area	1.67 m <sup>2</sup> (18 ft <sup>2</sup> )
Aerodynamic Drag Coefficient	0.33



Specifications Applicable to Hybrid Vehicle

Flywheel:

Rotor Weight	15.4 Kg (34 lbs)
Total Weight, Enclosed Module	22.7 Kg (50 lbs)
Total Stored Energy	1 Kwh
Available Stored Energy	0.75 Kwh
Battery Weight	363 Kg (800 lbs)
Battery Stored Energy @ 5 Kw Rate	9.8 Kwh

Specifications Applicable to All-Battery Electric Vehicle

Battery Weight	385 Kg (850 lbs)
Battery Stored Energy @ 5 Kw Rate	10.9 Kwh
Battery Stored Energy @ 20 Kw Rate	6 Kwh

C. DEFINITIONS

Nomenclature for Calculations and Discussion

A	acceleration	T	time duration
$\bar{A}$	area	V	velocity
B	battery	W	weight
$C_D$	drag coefficient	$W^*$	equivalent weight (includes inertia effect of rotating parts)
D	distance	X	range
E	energy	g	gravitational constant
$\bar{E}$	specific energy	$\alpha$	ratio
F	force	$\beta$	increment
$K_R$	rolling resistance coefficient	$\eta$	efficiency
L	losses	$\theta$	grade angle
P	power	$\phi$	fraction of stored energy
$\bar{P}$	specific power		
R	road		
$F_R$	rolling resistance force		

Subscripts:

- b battery
- f flywheel
- ℓ losses
- r road
- R rolling resistance
- D drag
- G gradient
- i inertia

Example of Use of Symbols:

The specific energy of the battery, but expressed as the value as delivered to the road is denoted as:  $\bar{E}_{br}$ .

The corresponding specific energy of the battery, but expressed as the value at the battery itself is:  $\bar{E}_{bb}$

Level-Road Power and Energy Requirements

a) Rolling Resistance Force. An average rolling resistance coefficient of 12 lbs force per 1000 lbs of car test weight has been assumed. This is compared with a value of 18 for present-day gasoline cars<sup>10</sup> and less than 10 for experimental electric vehicles.<sup>4</sup> While the rolling resistance force in actual practice has been found to rise as a weak function of vehicle velocity, it may be regarded as nearly constant over a speed range of 0 to 55 mph.

The total rolling resistance for the specified vehicles of 2400 lbs test weight is thus about 29 lbs force. This rolling resistance includes friction losses of rear axle gearing, wheel bearings, and tire rolling resistance.

b) Aerodynamic Drag Force. The air drag force, in pounds, is defined by the following expressions:

$$F_D = .002558 C_D \bar{A} V^2, \text{ where} \quad (\text{ref. 18})$$

$C_D$ , Zero yaw angle drag coefficient, = 0.33

$\bar{A}$ , projected frontal area = 18 sq. ft.

$V$ , velocity, miles per hour.

For the specified vehicles, this simplifies to:

$$F_D = .001520 V^2.$$

The drag coefficient used is typical of the profile of compact low-drag vehicles such as the Citroen.<sup>19</sup>

- c) Power and Energy Requirements. The total level-road tractive resistance force is the sum of the rolling and air resistance forces at any given velocity. Net energy requirements are equal to force times distance, and net power requirements are computed as force times velocity.

Table 15 gives the level-road power requirements for the specified hybrid and all-battery cars, over a range of velocities from zero to 60 mph.

TABLE 15

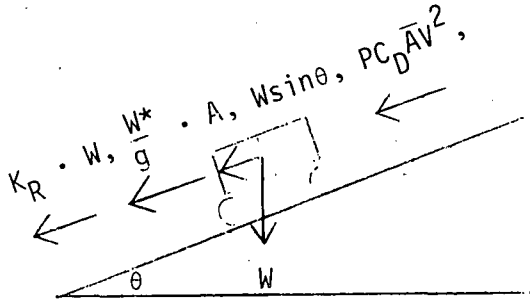
<u>Velocity</u> <u>Miles per hour</u>	<u><math>F_R + F_D</math></u> <u>Pounds, force</u>	<u>Road Load Power*</u> <u><math>P_r</math></u> <u>Kilowatts</u>
10	30.3	.60
15	32.2	.96
20	34.9	1.39
25	38.3	1.90
30	42.5	2.54
35	44.0	3.06
40	53.1	4.22
45	59.6	5.33
50	66.8	6.64
55	74.8	8.18
60	83.5	9.96

\*Required at output shaft of traction motor. Includes differential gearing losses.

General Expressions for Force, Energy, Power, and Range

The foregoing discussion was limited to the special case of steady-state, level-road travel. General expressions for vehicle motion when acceleration and hill climbing are involved are set forth below:

Summation of Forces:



Drag Force,  $F_D = .002558 C_D \bar{A} \cdot V^2$

Rolling Resistance,  $F_R = K_R \cdot W$

Inertia Force,  $F_i = \pm \frac{W^*}{g} \cdot A$  (a)

Gradient Force,  $F_G = \pm W \sin \theta$  (b)

Gradient, % = 100 tan  $\theta$

In general,  $F_D + F_R \pm F_G \pm F_i = \Sigma F$

At any velocity,  $V = \int_{T_0}^T A dt$

Instantaneous Power =  $P(t) = V \cdot \Sigma F$

Energy, E, used in Time, T, =  $E(t) = \int_{T_0}^T P(t) dt$

Range, X, in time, T, =  $X(t) = \int_{T_0}^T V dt$

Notes:

(a) An equivalent weight,  $W^*$ , is generally used in the mass term when computing the force to accelerate a vehicle. This equivalent weight includes an allowance for the inertia of rotating parts.  $W^* = 1.05 W$  approximately.

(b)  $\sin \theta$  is approximately the same as  $\tan \theta$  for the usual road gradients.

$F_G = \frac{\% \text{ grade } W}{100}$ , approximately.

### Urban Driving Cycles

A number of standardized driving cycles are used in this country at the present time. Some, such as the Federal Urban Test Procedure, are used primarily to evaluate the emissions and fuel economy of gasoline-powered standard automobiles.

The Society of Automotive Engineers (SAE) has developed two driving cycles specifically for the testing of electric cars. These are referred to as the SAE Metropolitan Area Driving Cycle and Residential Driving Cycle, respectively. A complete description of the driving schedules and test procedures is given in Reference (20). The designation is "Electric Vehicle Test Procedure - SAE J227."

The driving schedules are given as velocity-time profiles, intended to be driven over a level road in a repeated manner to ascertain the vehicle's range. Four distinctive operational modes are included: idle, acceleration, constant-velocity cruise, and deceleration. The characteristics of these driving cycles are given in Table 16 and Figure 31. Note that the two velocity-time schedules are identical, except for a period of higher cruising speed (45 mph vs. 30 mph) in the Metropolitan cycle.

### Battery Relationships

A characteristic of electrical storage batteries is that the available stored energy depends upon the rate at which that energy is withdrawn. At low power levels, lead-acid batteries can deliver two to three times the energy that is available at high power.

Figure 32 is a plot of the specific power vs. specific energy relationship of state-of-the-art lead acid batteries. This curve is the maximum performance limit of the lead-acid "band" of Figure 1, Vol. I, and hence may be representative of improved near-term lead-acid technology. Note that Figure 32 has been plotted with linear rather than logarithmic coordinates, to facilitate use in selecting values for computation.

TABLE 16  
ELECTRIC VEHICLE TEST PROCEDURE - SAE J277  
(Reference: SAE Handbook, 1976 Edition)

TEST SCHEDULE FOR METROPOLITAN AREA DRIVING CYCLE

<u>Mode</u>	<u>Average Acceleration, mph/sec</u>	<u>Time, sec</u>	<u>Cumulative Time, sec</u>
Idle	0	20	20
0-30 mph	2.14	14	34
30 mph constant	0	15	49
30-15 mph	-1.37	11	60
15 mph constant	0	15	75
15-45 mph	1.20	25	100
45 mph constant	0	21	121
45-20 mph	-1.19	21	142
20-0 mph	-2.50	8	150
Repeat Cycle	(Distance, .996 miles)		

TEST SCHEDULE FOR RESIDENTIAL DRIVING CYCLE

<u>Mode</u>	<u>Average Acceleration, mph/sec</u>	<u>Time, sec</u>	<u>Cumulative Time, sec</u>
Idle	0	20	20
0-30 mph	2.14	14	34
30 mph constant	0	15	49
30-15 mph	-1.37	11	60
15 mph constant	0	15	75
15-30 mph	1.20	12.5	87.5
30 mph constant	0	46.5	134
30-20 mph	-1.20	8	142
20-0 mph	-2.50	8	150
Repeat Cycle	(Distance, .858 miles)		

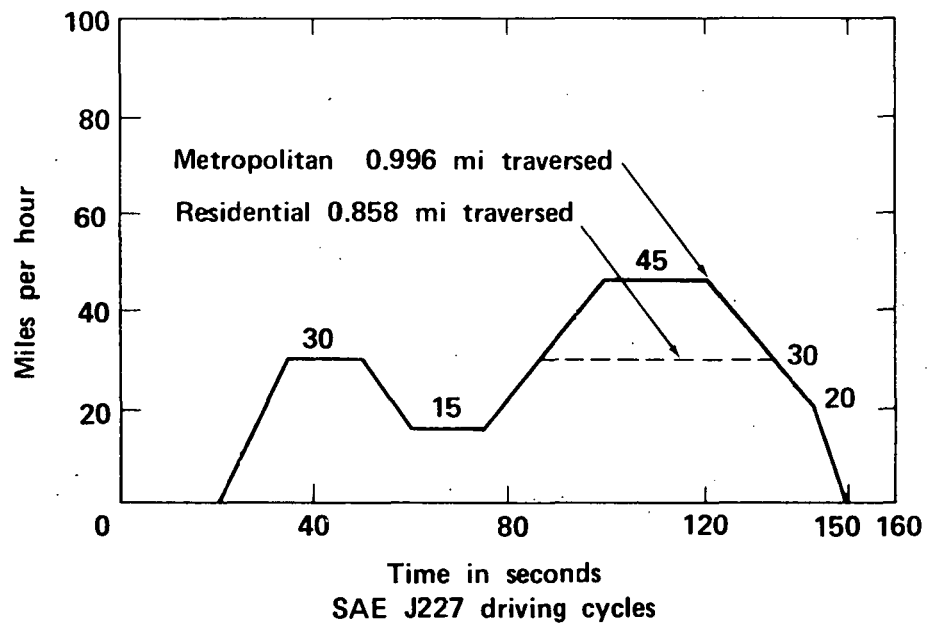


Fig. 31. Driving cycle profiles.

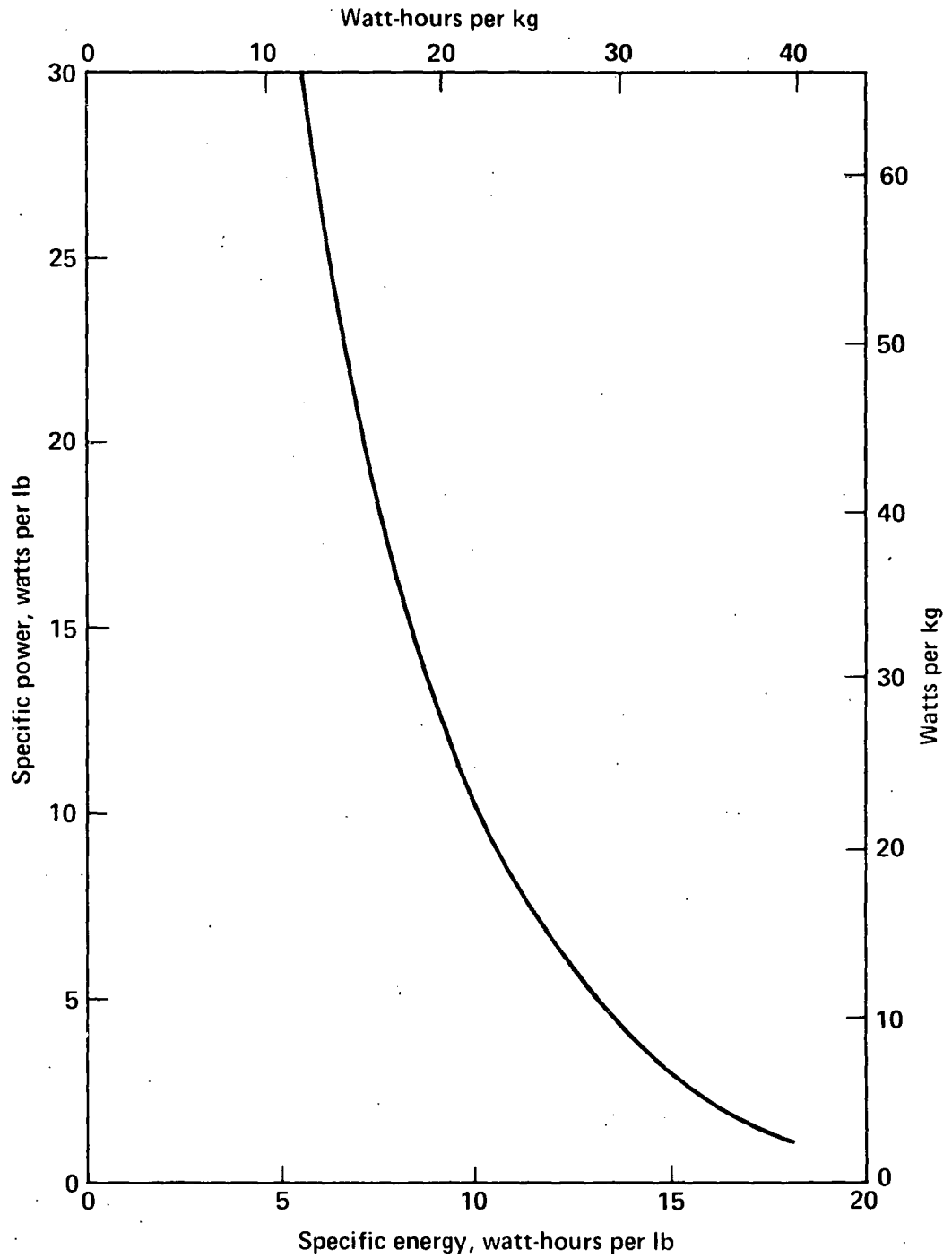


Fig. 32. Typical lead-acid battery characteristics.



### Efficiency Factors

(a) Power Train Efficiency. Once the road load requirements have been determined, the demands upon the energy storage sub-systems may be computed providing the efficiencies of the power train are known. The efficiencies of such elements as traction motors and gearing will vary continuously as a function of speed and applied load. Precise modelling of the vehicle's characteristics would require the faithful representation of these variable efficiencies. However, for these initial overview calculations, we have chosen to use an assumed fixed average value for the power train efficiency.

- Hybrid Vehicle - The design and characteristics of the power transmission sub-system have been described in Section II of this Volume. The powertrain has a reasonably high efficiency because a portion of the drive energy is transmitted by mechanical gearing rather than being entirely through the traction motor. The traction motor itself maintains a good efficiency because it is sized for cruise power demands, and hence the normal loads are close to its rating point. An average efficiency of 82% has been assumed for the hybrid vehicle drive train.

As will be noted shortly, flywheel run-down losses have not been included in the 82% figure, but are separately accounted for in the calculations.

- All-Battery Electric Vehicle - An average powertrain efficiency of 72% has been assigned, largely associated with the traction motor and any speed-reducing gearing that may be required. This efficiency is typical of existing electric cars over the wide range of speeds and loads encountered.<sup>16</sup> Compared with the hybrid vehicle, efficiency

is reduced by the fact that the traction motor must be rated to transmit peak power, and thus runs most of the time in an inefficient part-load regime.

- Flywheel Run-Down and Miscellaneous Losses - Flywheel run-down losses, flywheel auxiliary loads, and control losses have been estimated as follows:

<u>Loss or Parasitic Load</u>	<u>Power in Watts</u>		
	<u>At Max. RPM</u>	<u>At Min. RPM</u>	<u>Ave. or Effective Value</u>
Flywheel Windage	100	30	65
Flywheel Bearings and Seals	200	50	125
Oil and Vacuum Pumps	---	--	80
Power Control Unit	---	--	50
Total Misc. Loss			<u>320</u>

#### D. CALCULATIONS

##### Vehicle Range at Constant Speed on a Level Road

- a) Hybrid Vehicle. The vehicle's range has been computed for two steady-state conditions, 30 mph and 55 mph. Power requirements at the input to the drive axle are taken from Table 15; these values are 2.54 Kw at a steady 30 mph and 8.18 Kw at 55 mph. Dividing these power levels by the power train efficiency of 0.82 gives the propulsion power requirements at the battery.

Battery energy must also offset the flywheel run-down and miscellaneous losses of 320 watts. An 82% efficiency is also assumed for the energy transfer from the battery to the flywheel.

The flywheel energy storage is not tapped during these light-load cruise modes, except to extend the range beyond that of the battery alone.

Once the power drain at the battery has been determined (3.49 Kw for a steady 30 mph), the battery's capacity at that drain rate can be ascertained by the use of Figure 32. Dividing the power by the battery weight (800 lbs) gives the power density (4.36 w/lb), which in turn fixes the battery's energy density (13.70 wh/lb). The energy storage of the battery is then 800 lbs times 13.7 or 10.96 Kwh.

Finally, the range may be calculated by the following relationship:

$$\text{Range (mi)} = \left( \frac{\text{Energy Available, Kwh}}{\text{Power Requirements, Kw}} \right) \left( \text{Velocity, } \frac{\text{mi}}{\text{hr}} \right)$$

At 30 mph, the hybrid vehicle has an estimated range of 101 miles.

At 55 mph, the range is reduced to 42 miles. The calculational steps are summarized in Table 17.

- b) All-Battery Electric Vehicle. The same procedure is used to compute the range for the all-battery vehicle. A different power train efficiency is used (72% assumed), but no flywheel run-down losses are involved. The ranges are found to be 99 miles and 36 miles, respectively, for constant speeds of 30 and 55 mph. The calculations are summarized in Table 18.

#### Vehicle Range Over SAE Driving Cycles

- a) Hybrid Vehicle. The driving cycles are divided into segments, according to the operational mode (idle, acceleration, cruise, deceleration). Periods of constant velocity driving are treated in a manner just described.

During periods of positive or negative acceleration, the instantaneous propelling force required on a level road is

$$F = F_R + F_D \pm F_i,$$

where the elements of force are the rolling resistance, air drag, and inertia force, respectively.

TABLE 17  
CALCULATION OF ESTIMATED RANGE  
FOR HYBRID VEHICLE (CONSTANT VELOCITY)

30 MPH

$P_r$ , Road Load Power, 2.54 kw (see Table 15)

$\eta$ , Power Train Efficiency = 0.82

$W_b$ , Battery Wt. = 800 lbs  $W_f$ , Flywheel Wt. = 50 lbs

$E_{ff}$ , Flywheel Energy = 750 wh

$P_{lf}$ , Flywheel losses = 320 w

$$P_{bb} = (P_r + P_{lf}) \div \eta = (2.54 + .32) \div 0.82 = 3.49 \text{ kw}$$

$$\bar{P}_{bb} = P_{bb} \div W_b = 3490 \div 800 = 4.36 \text{ w/lb}$$

$$\bar{E}_{bb} = 13.7 \text{ wh/lb from Figure 32}$$

$$E_{bb} = \bar{E}_{bb} \times W_b = 13.7 \times 800 = 10.96 \text{ kwh}$$

$$\text{Range} = \left[ \frac{(E_{bb} + E_{ff})\eta}{P_r + P_{lf}} \right] V, \text{ MPH} = \left[ \frac{(10.96 + 0.75)(0.82)}{2.54 + 0.32} \right] 30 = 101 \text{ miles}$$

55 MPH

$P_r$  = 8.18 kw, other data as above.

$$P_{bb} = (8.18 + .32) \div 0.82 = 10.37 \text{ kw}$$

$$\bar{P}_{bb} = 10370 \div 800 = 12.96 \text{ w/lb}$$

$$\bar{E}_{bb} = 9.1 \text{ wh/lb from Figure 32}$$

$$E_{bb} = 9.1 \times 800 = 7.28 \text{ kwh}$$

$$\text{Range} = \left[ \frac{(7.28 + 0.75)(0.82)}{8.18 + .32} \right] 55 = 42 \text{ miles}$$

TABLE 18  
CALCULATION OF ESTIMATED RANGE  
FOR BATTERY-ONLY VEHICLE (CONSTANT VELOCITY)

30 MPH

$P_r$ , Road Load Power 2.54 kw (see Table 15)

$\eta$ , Power Train Efficiency, 0.72

$W_b$ , Battery Wt. 850 lbs

Battery Data, Figure 32

$$P_{bb} = P_r \div \eta = 2.54 \div 0.72 = 3.53 \text{ kw}$$

$$\bar{P}_{bb} = P_{bb} \div W_b = 3.53 \div 850 = 4.2 \text{ w/lb}$$

$$\bar{E}_{bb} = 13.7 \text{ wh/lb from Figure 32}$$

$$E_{bb} = \bar{E}_{bb} \times W_b = 13.7 \times 850 = 11.64 \text{ kwh}$$

$$E_{br} = E_{bb} \times \eta = 11.64 \times 0.72 = 8.38 \text{ kwh}$$

$$\text{Range} = \frac{E_{br}}{P_r} \times V(\text{MPH}) = \frac{8.38}{2.54} \times 30 = 99 \text{ miles}$$

55 MPH

$$P_r = 8.18 \text{ kw}$$

$$\eta = 0.72$$

$$W_b = 850 \text{ lbs}$$

$$P_{bb} = 8.18 \div 0.72 = 11.36 \text{ kw}$$

$$\bar{P}_{bb} = 11.36 \div 850 = 13.4 \text{ w/lb}$$

$$\bar{E}_{bb} = 8.7 \text{ wh/lb}$$

$$E_{bb} = 8.7 \times 850 = 7.39 \text{ kwh}$$

$$E_{br} = 7.39 \times 0.72 = 5.32 \text{ kwh}$$

$$\text{Range} = \frac{5.32}{8.18} \times 55 = 36 \text{ miles}$$

Furthermore, the instantaneous road-load power requirements (or power absorption, in the case of regenerative braking) can be expressed as:

$$P_r = (F_R + F_D \pm F_i) V,$$

where  $V$  is the instantaneous velocity.

An integration of power with respect to time will yield the energy required to traverse each mode segment of the driving cycle.

Table 19 is a summary of the power and energy requirements for the SAE Metropolitan Area Driving Cycle. Each mode of the driving cycle is defined by its time boundaries, in seconds after the start of the cycle (refer to Table 16 and Figure 31). Negative changes of energy are listed for those modes where the negative energy from deceleration exceeds the positive energy requirements to overcome rolling and air resistance. These increments of negative energy are theoretically available for regenerative braking.

At the bottom of Table 19, positive and negative (propelling and braking) energies have been totaled. The algebraic sum of these totals is the net energy to be supplied over the driving cycle if there were no vehicle system losses. In actual practice, of course, the energy supplied by the vehicle's energy storage system would be larger than the positive value shown, and the amount recovered by the regenerative braking process would be less than the negative value listed. The next step in the calculation will be to adjust for the power train efficiency and other identified losses.

Table 20 is similar to 19, except it is for the SAE Residential Driving Cycle. The net energy requirement for this cycle is less than for the Metropolitan Cycle because a lower maximum speed is attained in the last cruising mode.

TABLE 19  
 POWER AND ENERGY REQUIREMENTS\* FOR  
 SAE METROPOLITAN AREA DRIVING CYCLE  
 (2400-1b Test Weight Vehicle)

<u>Mode</u> <u>Cumulative</u>	<u>Time</u> <u>Δ</u>	<u>Power</u> <u>Ave.</u>	<u>kw</u> <u>Peak</u>	<u>Energy,</u> <u>Δ</u>	<u>whr</u> <u>Cumulative</u>
0			-		-
	20	-	(Idle)	-	-
20			-		-
	14	8.40		32.68	
34			17.21		32.68
	15	2.54		10.58	
49			-6.87		43.26
	11	-5.33		-16.28	
60			-3.79		26.98
	15	.96		4.00	
75			5.07		30.98
	25	10.97		76.16	
100			17.69		107.14
	21	5.33		31.09	
121			-6.90		138.23
	21	-5.80	-4.07	-33.82	
142			-10.03		104.41
	8	-5.07		-11.27	
150			-		93.18
			Required Energy	(+154.51)	
			Regenerative Energy	(- 61.37)	
			Algebraic Sum	+ 93.14	

\*Power and energy at vehicle's drive axle

TABLE 20  
 POWER AND ENERGY REQUIREMENTS\* FOR  
 SAE RESIDENTIAL DRIVING CYCLE  
 (2400-lb Test Weight Vehicle)

<u>Mode Cumulative</u>	<u>Time Δ</u>	<u>Power Ave.</u>	<u>kw Peak</u>	<u>Energy, Δ</u>	<u>whr Cumulative</u>
0			-		-
	20	-	(Idle)	-	
20			-		-
	14	8.40		32.68	
34			17.21		32.68
	15	2.54		10.58	
49			-6.87		43.26
	11	-5.33		-16.28	
60			-.379		26.98
	15	.96		4.00	
75			5.07		30.98
	12.5	7.84		27.22	
87.5			10.76		58.20
	46.5	2.54		32.81	
134					91.01
	8	4.855		-10.79	
142			-4.07		80.22
			-10.03		
	8			-11.27	
150			0		68.95
				Required Energy	(+107.29)
				Regenerative Energy	(- 38.34)
				Algebraic Sum	+ 68.95

\*Power and Energy at Vehicle's drive axle



Table 21 is a summary of the calculations which lead to a determination of the hybrid vehicle's range. Basically, the computational steps are:

- Modify the theoretical propelling and braking energies by the drive train efficiency of 82%;
- Account for other losses over the driving cycle, such as the flywheel run-down losses and other parasitic loads and losses (which ultimately come from the battery) with a battery-to-flywheel efficiency of 82%;
- Apportion by trial the fractional depletion of energy from the battery and flywheel, respectively;
- Iterate the process such that the battery and the flywheel are exhausted simultaneously (a design goal for the hybrid system);
- Calculate the range by dividing the distance travelled per cycle by the fraction of the stored energy discharged per cycle.

In the calculations shown in Table 21, these rules were observed:

- The battery drain rate was arbitrarily limited so as to obtain a favorable energy storage capacity from it. All peak loads (during the accelerations) are supplied by the flywheel. Demands on the battery are thus limited to around 4 Kw, while peaks of over 20 Kw are accommodated by the combined energy storage sub-systems.
- All regenerative braking energies were routed to the flywheel.
- All miscellaneous losses, such as flywheel windage, are ultimately made up from the battery's energy storage. This make-up from the battery is accomplished during periods of idle and low power demands.

TABLE 21  
CALCULATIONS FOR HYBRID VEHICLE RANGE  
OVER SAE J227 DRIVING CYCLES

Step	Metropolitan Area Cycle	Residential Cycle	Units
(1) Find Energy Storage Requirement			
- Req'd. Road Energy ÷ 0.82	188.4	130.8	wh
- Regenerative Energy x 0.82	-50.3	-31.4	wh
- Flywheel Losses ÷ 0.82	16.2	16.2	wh
Total Energy/Cycle, $E_{total}$	154.3	115.6	wh
<u>First Approximations:</u>			
(Battery Storage Capy. from Power Density)			
(2) Ave. $P_b = (E_{total}) \left( \frac{3600}{150 \text{ sec}} \right)$	3703*	2774*	w
(3) $\bar{P}_b = \frac{P_b}{800 \text{ lb}}$	4.6	3.5	w/lb
(4) $\bar{E}_b$ , from Figure 16	13.5	14.5	wh/lb
(5) $E_b = (800 \text{ lbs})(\bar{E}_b)$	10,800	11,600	wh
(6) Fraction of Battery Discharged Per Cycle:			
$\phi = \frac{E_{total \text{ Per Cycle}}}{E_b \text{ Capacity}}$	0.0143	0.00997	-
(7) Provisional Energy Per Cycle From Flywheel:			
$\Delta E_f = 750\phi$	10.7	7.5	wh
(8) Find New Value for Energy/Cycle from Battery:			
$\Delta E_b = E_{total} - \Delta E_f$	143.6	108.1	wh

\*For first iteration assumes  $\Delta E_b = E_{total} = 154.3 \text{ wh}$

TABLE 21, Continued

<u>Iterate, Steps (2) - (8):</u>	<u>Metropolitan Area Cycle</u>	<u>Residential Cycle</u>	<u>Units</u>
(2) $P_b = (\Delta E_b) \left( \frac{3600}{150 \text{ sec}} \right)$	3446	2594	w
(3) $\bar{P}_b = \frac{P_b}{800}$	4.31	3.24	w/lb
(8) $\text{New } \Delta E_b = E_{\text{total}} - \text{New } \Delta E_f$	144.5	108.7	wh
<u>Results of Subsequent Iteration:</u>			
(7) $\emptyset = \emptyset_f$ (Value Closes by Iteration)	0.0133	0.00918	-
<u>Calculate Range:</u>			
(9) Distance Per Cycle, $\Delta X$	0.996	0.858	mi
(10) Range, $X = \frac{\Delta X}{\emptyset}$	75	94	mi

The range potential over the Metropolitan Cycle is estimated to be 75 miles, and over the Residential Cycle, 94 miles.

b) All-Battery Electric Vehicle. The same power and energy requirements at the drive axle (see Tables 19 and 20) were assumed for the all-battery vehicle. The range for the all-battery vehicle is also computed by dividing the miles traveled per cycle by the fraction of stored energy dissipated per repeated cycle. However, the intervening computational steps differ from the hybrid vehicle calculation in the following important ways:

- The battery must now furnish all of the peak loads, which reach approximately 25 Kw at the battery. The periods of high load seriously diminish the battery's storage capacity (Refer to Figure 32).
- A different value for power train efficiency has been assumed (0.72 vs. 0.82 for the hybrid). However, there are no flywheel run-down and other flywheel-associated losses to supply.
- No regenerative braking was assumed (although some small benefit, subject to charging rate limitations, could no doubt be incorporated). However, it was assumed that the battery would not have to supply any energy during the deceleration modes.

The estimated range potential of the all-battery vehicle is 34 miles over the Metropolitan Cycle and 51 miles over the Residential Cycle.

#### E. RANGE CALCULATION SUMMARY

Table 22 summarizes the touring range potentials estimated for the two vehicle types and for differing driving schedules:

TABLE 22  
Estimated Ranges for Hybrid  
and All-Battery Electric Vehicles  
(Two-Passenger Urban Vehicles, 2400-lb Test Weight)

<u>Driving Schedule</u> (All Over Level Roads)	<u>Range, Kilometers (miles)</u>	
	<u>Hybrid</u>	<u>All-Battery</u>
Constant 30 mph	163 (101)	159 (99)
Constant 55 mph	68 (42)	57 (36)
SAE Metropolitan Cycle	121 (75)	55 (34)
SAE Residential Cycle	151 (94)	82 (51)

#### F. GRADE AND ACCELERATION PERFORMANCE

##### Transient Performance

The estimated hybrid vehicle acceleration capability is portrayed in Figure 33. This performance is considerably above that normally associated with electric vehicles. The acceleration shown in Figure 33 is obtained utilizing flywheel power only. One of the properties of a flywheel is, that virtually any desired power level can theoretically be drawn for a short time. There would be practical limitations, of course, imposed by the rating of the power train.

##### Distance Capability on Grades

The capability of the hybrid vehicle to negotiate various distances of road gradients is shown in Figure 34. The basis is an assumed 750 wh available from the flywheel together with battery power which is arbitrarily limited to 5 Kw.

Grade climbing at constant velocity represents a steady-state energy flow. Calculations for the curves in Figure 34 were performed by a procedure similar to the level-road constant-velocity range calculations, except that the road loads were higher and the flywheel participated. The range in this case was determined by the exhaustion of the flywheel's available energy.

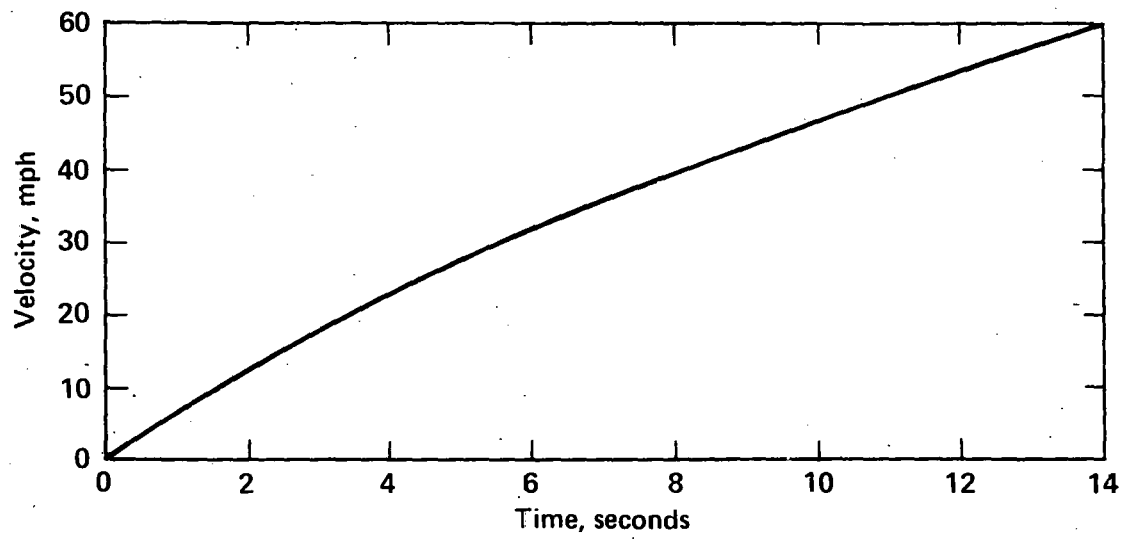


Fig. 33. Hybrid vehicle acceleration performance.

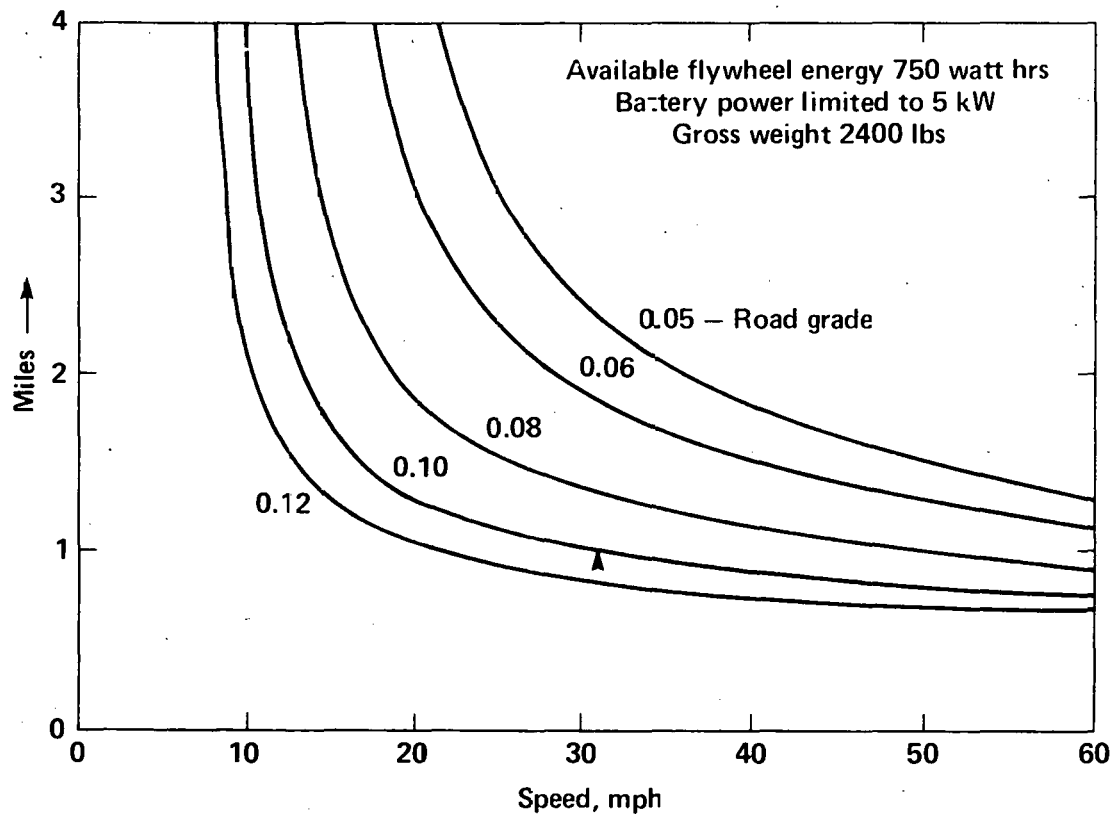


Fig. 34. Grade and distance capability of flywheel system with low power assist from battery.

## REFERENCES

1. C. J. Anderson et. al., An Assessment of U.S. Energy Options for Project Independence, Lawrence Livermore Laboratory, Report UCRL-51638 (1974).
2. Energy Statistics, U.S. Dept. of Transportation DOT TSC OST 75-33 (August 1975).
3. C. J. Anderson, Supply and Demand of Fuel Sources for Automobiles, Lawrence Livermore Laboratory, Report UCRL-78066 (Preprint), May 1976
4. R. S. McKee, et. al., Sundancer, A Test Bed Electric Vehicle, SAE 720188 (January 1972).
5. "1975 Automobile Facts and Figures", Motor Vehicle Manufacturers Assoc.
6. M. Beller, Editor, Sourcebook for Energy Assessment, Brookhaven National Laboratory, Report BNL-50483 (December 1975).
7. Gould Battery Handbook, Gustav A. Mueller, Ed., Gould Inc.
8. C. L. Montell, Batteries and Energy Systems, McGraw-Hill, p. 124.
9. Impact of Future Use of Electric Cars in the Los Angeles Region, General Research Corporation, NTIS PB-238878.
10. The Automobile and Air Pollution, A Plan for Progress, Report of the Panel on Electrically Powered Vehicles, U.S. Department of Commerce, (October 1967).
11. Highway Statistics 1973, Federal Highway Administration, U.S. Department of Transportation.
12. F. Kalhammer, "Energy Storage: Incentives and Prospects for its Development", presented to Amer. Chem. Soc. (Atlantic City, September 12, 1974).
13. P. A. Nelson, A. A. Chilenskis and R. K. Steunenber, The Need for Development of High Energy Batteries for Electric Automobiles, Argonne National Laboratory, Report ANL-8075 Draft (January 1974).
14. L. G. O'Connell, et. al., The Lithium-Water-Air Battery: A New Concept for Automotive Propulsion, Lawrence Livermore Laboratory, Report UCRL-51811 (May 1, 1975).
15. Roy A. Renner, Consulting Engineer, Livermore Ca., private communication (February 1976).



16. L. R. Foote and J. F. Hough, "An Experimental Battery Powered Ford Cortina Estate Car", Society of Automotive Engineers, Paper No. 700024 (January 1970).
17. From CPU to Software, Intel Corp. (1974).
18. D. M. Tenniswood et. al., Minimum Road Loads for Electric Cars, SAE Paper No. 670117 (January 1976).
19. A. Morelli, Body Shapes of Minimum Drag, SAE Paper No. 760186 (February 1976).
20. SAE Handbook, 1972 Edition, Society of Automotive Engineers.

DISTRIBUTION LIST -- UCID-17098

External:

ERDA Headquarters  
20 Massachusetts Avenue  
Washington D.C. 20545

- (1) George Pezdirtz
- (5) George Chang
- (4) John Brogan
- (1) J. Friedericic

Airesearch Manufacturing Company of Calif.  
2525 West 190 Street  
Torrance, Ca. 90509

- (1) A. E. Raynard
- (1) B. H. Rowlett
- (3) G. Souva
- (1) A. Morgan
- (1) J. Friedericic

Roy A. Renner, Consultant  
2020 Research Drive  
Livermore, Ca. 94550

Stanley E. Warner, Consultant  
21273 Tyee Street  
Castro Valley, Ca. 94546

Internal:

R. Batzel/D. Sewell, L-1  
K. Street, L-209  
G. Werth, L-216  
C. J. Anderson, L-216  
W. Arnold, L-123  
E. Behrin, L-216  
J. W. Bell, L-161  
B. J. Berger, L-216  
I. Y. Borg, L-216  
T. T. Chiao, L-421  
J. F. Cooper, L-426  
R. L. Cooper, L-216  
D. D. Davis, L-216  
D. Epps, L-24  
F. Holzer, L-209  
T. Jeffries, L-216  
P. H. Moulthrop, L-216  
H. C. McDonald, L-161  
R. L. Peterson, L-438  
L. G. O'Connell, L-216  
W. J. Ramsey, L-216  
B. Rubin, L-216  
R. G. Stone, L-123  
A. J. Stripeika, L-151  
S. S. Sussman, L-216  
R. Thornton, L-216  
H. Timourian, L-216  
R. L. Ward, L-216  
E. A. LaFranchi, L-151  
E. R. McClure, L-383  
  
T.I.D. (15)  
Energy & Resource Planning  
group (25)  
  
T.I.C. Oak Ridge (27)

NOTICE

"This report was prepared as an account of work sponsored by the United States Government. Neither the United States nor the United States Energy Research & Development Administration, nor any of their employees, nor any of their contractors, subcontractors, or their employees, makes any warranty, express or implied, or assumes any legal liability or responsibility for the accuracy, completeness or usefulness of any information, apparatus, product or process disclosed, or represents that its use would not infringe privately-owned rights."

Printed in the United States of America  
 Available from  
 National Technical Information Service  
 U.S. Department of Commerce  
 5285 Port Royal Road  
 Springfield, VA 22161  
 Price: Printed Copy \$ : Microfiche \$2.25

<u>Page Range</u>	<u>Domestic Price</u>	<u>Page Range</u>	<u>Domestic Price</u>
001-025	\$ 3.50	326-350	10.00
026-050	4.00	351-375	10.50
051-075	4.50	376-400	10.75
076-100	5.00	401-425	11.00
101-125	5.25	426-450	11.75
126-150	5.50	451-475	12.00
151-175	6.00	476-500	12.50
176-200	7.50	501-525	12.75
201-225	7.75	526-550	13.00
226-250	8.00	551-575	13.50
251-275	9.00	576-600	13.75
276-300	9.25	601-up	*
301-325	9.75		

\* Add \$2.50 for each additional 100 page increment from 601 to 1,000 pages; add \$4.50 for each additional 100 page increment over 1,000 pages.

*Technical Information Department*

**LAWRENCE LIVERMORE LABORATORY**

University of California | Livermore, California | 94550